Journal of Financial Economics 117 (2015) 558–584

Contents lists available at ScienceDirect

Journal of Financial Economics

journal homepage: www.elsevier.com/locate/jfec

The risk premia embedded in index options ☆

Torben G. Andersen [a], Nicola Fusari [b,*], Viktor Todorov [a]

[a] Department of Finance, Kellogg School of Management, Northwestern University, Evanston, IL 60208, United States
[b] The Johns Hopkins University Carey Business School, Baltimore, MD 21202, United States

ARTICLE INFO

Article history:
Received 25 August 2014
Received in revised form
3 December 2014
Accepted 16 December 2014
Available online 12 June 2015

JEL classification:
C51
C52
G12

Keywords:
Option pricing
Risk premia
Jumps
Stochastic volatility
Return predictability
Risk aversion
Extreme events

ABSTRACT

We study the dynamic relation between market risks and risk premia using time series of index option surfaces. We find that priced left tail risk cannot be spanned by market volatility (and its components) and introduce a new tail factor. This tail factor has no incremental predictive power for future volatility and jump risks, beyond current and past volatility, but is critical in predicting future market equity and variance risk premia. Our findings suggest a wide wedge between the dynamics of market risks and their compensation, which typically displays a far more persistent reaction following market crises.

1. Introduction

Equity markets are subject to pronounced time variation in volatility as well as abrupt shifts, or jumps. Moreover, these risk features are related in intricate ways, inducing a complex equity return dynamics. Hence, the markets are incomplete, and derivative securities, written on the equity index, are non-redundant assets. This

☆ We are grateful to Bill Schwert (the editor), David Bates (the referee), and Snehal Banerjee, Geert Bekaert, Peter Carr, Anna Cieslak, Bjorn Eraker, Kay Giesecke, Ravi Jagannathan, Bryan Kelly [our discussant at the National Bureau of Economic Research (NBER) meeting], Robert Merton, Toby Moskowitz, Lasse Pedersen, Sergio Rebelo, Myron Scholes, Ivan Shaliastovich (our discussant in Montreal, Canada), Allan Timmermann, Jonathan Wright, and Liuren Wu, as well as seminar participants at Kellogg School of Management, Northwestern University, Duke University, the 'Montreal 2013 Econometrics Conference: Time Series and Financial Econometrics,' the 40th Annual Meeting of the Danish Econometric Society, Sandbjerg, Denmark, the European University Institute, Florence, Italy 2013 Workshop on 'Measuring and Modeling Financial Risk and High Frequency Data', the 2013 'International Conference in Financial Econometrics' at Shandong University, Jinan, China, the '40 Years after the Black-Scholes-Merton Model' conference at the Stern School of Business (October 2013), the NBER Asset Pricing Meeting at Stanford University (November 2013), Georgia Tech, Boston University, Stanford University, the Insight Award Conference, sponsored by AQR Capital Management, Greenwich, Connecticut (April 2014), the 2014 Annual Society for Financial Econometrics (SoFiE) Meeting, Toronto, Canada, the 2014 Australasian Econometric Society Meetings, Tasmania, Australia, the 2014 NBER Summer Institute Forecasting, and Empirical Methods Meeting, and the 2014 European Finance Association (EFA) meeting, Lugano, Switzerland, for helpful comments. Torben G. Andersen gratefully acknowledges support from CREATES, Center for Research in Econometric Analysis of Time Series (DNRF78), funded by the Danish National Research Foundation. Viktor Todorov's work was partially supported by National Science Foundation Grant SES-0957330.

* Corresponding author. Tel.: +1 410 234 9411; fax: +1 410 234 9439.
E-mail addresses: t-andersen@northwestern.edu (T.G. Andersen), nicola.fusari@jhu.edu (N. Fusari), v-todorov@northwestern.edu (V. Todorov).

http://dx.doi.org/10.1016/j.jfineco.2015.06.005
0304-405X/

partially rationalizes the rapid expansion in the trading of contracts offering distinct exposures to volatility and jump risks. From an economic perspective, it suggests that derivatives data contain important information regarding the risk and risk pricing of the underlying asset. Recent evidence, exploiting parametric models, e.g., Christoffersen, Jacobs, and Ornthanalai (2012) and Santa-Clara and Yan (2010), or nonparametric techniques, e.g., Bollerslev and Todorov (2011), finds the pricing of jump risk, implied by option data, to account for a significant fraction of the equity risk premium.

Standard no-arbitrage and equilibrium-based asset pricing models imply a tight relation between the dynamics of the options and the underlying asset. This arises from the assumptions concerning the pricing of risk in the no-arbitrage setting and the endogenous pricing kernels implied by the equilibrium models. A prominent example is the illustrative double-jump model of Duffie, Pan, and Singleton (2000) in which the return volatility itself follows an affine jump diffusion. In this context, the entire option surface is governed by the evolution of market volatility, i.e., the dynamics of all options is driven by a single latent Markov (volatility) process.

Recent empirical evidence reveals, however, that the dynamics of the option surface is far more complex. For example, the term structure of the volatility index (VIX) shifts over time in a manner that is incompatible with the surface being driven by a single factor, see, e.g., Johnson (2012). Likewise, Bates (2000) shows that a two-factor stochastic volatility model for the risk-neutral market dynamics provides a significant improvement over a one-factor version. Moreover, Bollerslev and Todorov (2011) find that even the short-term option dynamics cannot be captured adequately by a single factor as the risk-neutral tails display independent variation relative to market volatility, thus driving a wedge between the dynamics of the option surface and the underlying asset prices.

The objective of our paper is to characterize the risk premia, implied by the large panel of Standard & Poor's (S&P) 500 index options, and its relation with the aggregate market risks in the economy. As discussed in Andersen, Fusari, and Todorov (2015), the option panel contains rich information both for the evolution of volatility and for jump risks and their pricing. Consequently, we let the option data speak for themselves in determining the risk premium dynamics and discriminating among alternative hypotheses regarding the source of variation in risk and risk pricing.

The standard no-arbitrage approach starts by estimating a parametric model for the evolution of the underlying asset price. Risk premia are introduced through a pricing kernel, which implies that risk compensation is obtained through parameter shifts. This ensures, conveniently, that the risk-neutral dynamics remains within the same parametric class entertained for the statistical measure. However, this approach tends to tie the equity market and option surface dynamics closely together. The equity risk premia are typically linear in volatility. In contrast, we find the options to display risk price variation that is largely unrelated to, and effectively unidentifiable from, the underlying asset prices alone.

This motivates our reverse approach of directly estimating a parametric model for the risk-neutral dynamics exclusively from option data along with no-arbitrage restrictions based on nonparametric model-free volatility measures constructed from high-frequency data on the underlying asset. In this manner, we avoid letting a (possibly misspecified) parametric structure for the $\mathbb{P}$-dynamics impact the identification of option risk premia. Our goal is to synthesize the option surface dynamics in a low-dimensional state vector without imposing ad hoc restrictions based on the actual return dynamics and then proceed to explore the risk premia dynamics by combining the extracted state vector with high- and low-frequency data on the equity index.

Following Andersen, Fusari, and Todorov (2015), we specify a general parametric model for the risk-neutral return dynamics that allows for a separate left tail jump factor to impact the volatility surface. Simultaneously, we include two distinct volatility factors and accommodate co-jumps between returns and volatility as well as return asymmetries induced by (negative) correlation between both diffusive and jump innovations. Moreover, we explore both Gaussian and double-exponential specifications for the jump distributions. As such, we incorporate all major features stressed in prior empirical option pricing studies and allow for various novel features. We model the tail factor as purely jump-driven, with one component jointly governed by the volatility jumps and another independent of spot volatility. This feature allows the jump intensity to escalate, through so-called cross-excitation of the jumps, in periods of crises when price and volatility jumps are prevalent, thus amplifying the response of the jump intensity to major (negative) market shocks. The extended model remains within the popular class of affine jump-diffusion models of Duffie, Pan, and Singleton (2000) and exemplifies the flexibility of such models for generating intricate, yet analytically tractable, dynamic interactions between volatility and jump risks.

Any tractable and parsimonious parametric model is bound to suffer from some degree of misspecification. What is crucial for our analysis, however, is to avoid systematic biases in representing the information embedded in the option panel. We do this by allowing for a flexible state vector driving different components of the conditional risk-neutral return distribution. Most important, by introducing the left tail factor, we capture systematic variation in the corresponding part of the option surface, which is missed by traditional model specifications. One can view the time series realizations of our novel tail factor as a succinct quantification of dynamic features not accommodated by existing parametric asset pricing models.

Relative to Andersen, Fusari, and Todorov (2015), the system is generalized to allow the left tail factor to enter directly into the spot volatility process. In addition, all three state variables could impact the jump intensities. Consequently, we can explicitly test for the presence of the tail factor in volatility, and we can gauge the significance of the different state variables in driving separately the positive and negative jump intensities. Inference for the general model is feasible through the approach developed

in Andersen, Fusari, and Todorov (2015). However, we modify the criterion function by including a term minimizing not the squared, but the relative squared option pricing error across the sample. This reduces the weight assigned to turbulent periods when the bid–ask spreads increase sharply.

The estimation of the general system establishes that the left tail factor is an insignificant contributor to spot volatility, even if it is correlated with the level of volatility. Moreover, it has no presence in the right jump tail, while the left jump intensity is exclusively governed by the tail factor and the more volatile and less persistent of the volatility components. Overall, the tail factor improves the characterization of the option surface dynamics very significantly, both in- and out-of-sample. In particular, the new model no longer systematically undervalues out-of-the-money (OTM) put options following crises. Given the much improved fit to the option surface, our extended model provides a more suitable basis for studying the dynamics of the market risk premia.

Methodologically, the presence of the separately evolving tail factor implies that part of the risk premium dynamics cannot be captured by the volatility state variables driving the underlying asset price dynamics. This suggests that the tail factor can have predictive power for risk premia over and above spot volatility. This is what we find. Our tail factor is important for forecasting the variance risk premium in conjunction with one of the volatility components. In addition, the tail factor is significant in predicting excess market returns for horizons up to one year, and the volatility factors are insignificant. These findings rationalize why the variance risk premium is a superior return predictor relative to volatility itself, as shown in Bollerslev, Tauchen, and Zhou (2009). The key is the presence of a separate factor driving the left jump tail of the risk-neutral distribution. At the same time, the tail factor provides substantially better return forecasts than the variance risk premium, or any other standard return predictor, over our sample.

Importantly, while the new tail factor has predictive power for risk premia, it contains no incremental information regarding the future evolution of volatility and jump risks for the underlying asset relative to the traditional volatility factors. Hence, our findings indicate that option markets embody critical information about the market risk premia and its dynamics which is essentially unidentifiable from stock market data alone. Moreover, the option surface dynamics contains information that can improve the modeling and forecasting of future volatility and jump risks, but such applications necessitate an initial untangling of the components in the risk premia that are not part of the volatility process. Overall, our empirical results suggest that a wedge exists between the stochastic evolution of risks in the economy and their pricing, which typically has a far more persistent response to (negative) tail events than the former.

Our finding of a substantial wedge between the dynamics of the option and stock markets presents a challenge for structural asset pricing models. The standard exponentially affine equilibrium models with a representative agent equipped with Epstein-Zin preferences imply that the ratio of the risk-neutral and statistical jump tails is constant. On the contrary, the new factor, extracted from the option data, drives the risk-neutral left jump tail but has no discernable impact on the statistical jump tail. We conjecture that this wider gap between fundamentals and asset prices can be accounted for through an extension of the preferences via some form for time-varying risk aversion or ambiguity aversion, or both, toward extreme downside risk.

The rest of the paper is organized as follows. Section 2 describes the data. Section 3 presents our three-factor model, which, apart from the modeling of the jump distributions, encompasses most existing models in the empirical literature. Section 4 introduces the estimation methodology and discusses the parameter estimates. Section 5 explores model fit and presents different robustness checks. This analysis brings out some of the mechanisms behind the improved fit of our model. Section 6 is dedicated to an out-of-sample analysis. In Section 7, we exploit the estimation results to study the risk premium dynamics and its implication for return and variance predictability. Our findings are contrasted to corresponding predictability results implied by popular structural equilibrium models. Section 8 concludes. Details on various aspects of the analysis are collected in the Appendix. A number of additional robustness checks and further details on the estimation are provided in the Supplementary Appendix.

2. Data and preliminary analysis

We use European-style S&P 500 equity-index (SPX) options traded at the Chicago Board Options Exchange (CBOE). We exploit the closing bid and ask prices reported by OptionMetrics, applying standard filters and discarding all in-the-money options, options with time-to-maturity of less than seven days, and options with zero bid prices. For all remaining options, we compute the mid bid–ask Black-Scholes implied volatility (IV). The data span January 1, 1996 to April 23, 2013. They are further divided into an in-sample period covering January 1, 1996 to July 21, 2010 and an out-of-sample period July 22, 2010 to April 23, 2013. Following earlier empirical work, e.g., Bates (2000) and Christoffersen, Heston, and Jacobs (2009), we sample every Wednesday.[1] The in-sample period has 760 trading days, and the estimation is based on an average of 234 bid–ask quotes per day. The out-of-sample period contains 142 trading days and features a much higher number of active quotes at any time, so we exploit an average of 708 option contracts daily from this sample. The nonparametric estimate of volatility used for penalizing the objective function is constructed from one-minute data on the S&P 500 futures covering the time span of the options. The same data are used to construct measures of volatility and jump risks for the predictive regressions in Section 7. Finally, we employ the returns on the Standard & Poor's exchange-traded fund (SPDR) traded on the NYSE, which

[1] Due to extreme violations of no-arbitrage conditions, we replace October 8, 2008 with October 6, 2008.

Table 1
Relative number of contracts.

We report the percentage of option contracts that, on average, fall within the different combinations of moneyness and tenor for the indicated sample.

Moneyness	1996:1–2010:7		2010:7–2013:4	
	$\tau \le 60$	$\tau > 60$	$\tau \le 60$	$\tau > 60$
$m \le -3$	10.36	5.23	18.46	8.62
$m \in (-3, -1]$	12.34	11.89	12.31	11.03
$m \in (-1, 1]$	19.58	24.77	14.58	17.90
$m > 1$	8.71	7.13	10.34	6.76
All	50.98	49.02	55.69	44.31

tracks the S&P 500 index portfolio, and the three-month T-bill rate to proxy for the risk-free rate, when implementing these regressions.

2.1. The option panel

We denote European-style out-of-the-money option prices for the asset X at time t by $O_{t,k,\tau}$. Assuming frictionless trading in the options market and denoting with $\mathbb{Q}$ the risk-neutral measure, the option prices at time t are given as

$$O_{t,k,\tau} = \begin{cases} \mathbb{E}_t^{\mathbb{Q}}\left[e^{-\int_t^{t+\tau} r_s\, ds}(X_{t+\tau}-K)^+\right] & \text{if } K > F_{t,t+\tau}, \\ \mathbb{E}_t^{\mathbb{Q}}\left[e^{-\int_t^{t+\tau} r_s\, ds}(K-X_{t+\tau})^+\right] & \text{if } K \le F_{t,t+\tau}, \end{cases} \tag{1}$$

where τ is the tenor of the option, K is the strike price, $F_{t,t+\tau}$ is the futures price for the underlying asset at time t referring to date $t+\tau$, for $\tau > 0$, $k = \ln(K/F_{t,t+\tau})$ is the log-moneyness, and r_t is the instantaneous risk-free interest rate. Finally, we denote the annualized Black-Scholes implied volatility corresponding to the option price $O_{t,k,\tau}$ by $\kappa_{t,k,\tau}$. This merely represents an alternative notational convention, as the Black-Scholes implied volatility is a strictly monotone transformation of the ratio $e^{r_{t,t+\tau}} O_{t,k,\tau}/F_{t,t+\tau}$, where $r_{t,t+\tau}$ denotes the risk-free rate over the period $[t, t+\tau]$.

The empirical work explicitly accounts for measurement error in the option prices. We denote the average of the bid and ask quotes (expressed in Black-Scholes implied volatility units) by $\overline{\kappa}_{t,k,\tau}$, and we view this as a noisy observation of underlying value. To the extent the measurement errors are not strongly correlated across a large fraction of the surface, we improve the efficiency of the inference by incorporating the full option cross section in our estimation and testing procedures, effectively averaging out idiosyncratic observation errors. The size of the spread varies over time and is positively correlated with the volatility level. In addition, systematic differences exist in the relative spread across moneyness. For example, the spread is about 8% of the mid-quote for deep OTM puts, on average, implying that a typical implied volatility reading of 40% is associated with bid and ask quotes of 38.4% and 41.6%, respectively. Similarly, for an IV of 18% for at-the-money (ATM) options, the quotes are generally around 17.6–18.4%, and a typical set of quotes for far OTM calls are 18.8–21.2% for a midpoint value of 20%.

The options underlying the IV surface are highly heterogeneous in terms of moneyness and tenor across time. To facilitate comparison, we create a uniform set of regions based on the option characteristics. We define the volatility-adjusted moneyness, m, at time t for tenor τ, by standardizing the log-moneyness with the ATM IV,

$$m = \frac{\ln(K/F_{t,t+\tau})}{\kappa_{t,0,\tau} \cdot \sqrt{\tau}}. \tag{2}$$

Table 1 shows how the observations in our sample are distributed across the option surface. The four regions of moneyness represent deep OTM put options, OTM put options, ATM options, and OTM call options, and the two categories for time-to-maturity provide a rough split into short- versus long-dated options. Not surprisingly, there is particularly good coverage for ATM options, which represent over 44% of the in-sample observations. The quotes for the OTM call options are somewhat limited and amount to almost 16% of the total options quotes, roughly matching the proportion of deep OTM put options.

In the out-of-sample period, the daily number of active quotes is much higher, especially for deep OTM options. Because we would like to compare model performance across the two samples, we have truncated the set of OTM options included in the recent period to lie within the boundaries of -7.1 for the puts and 2.4 for the calls. These cutoffs correspond to the average minimum and maximum moneyness of the option quotes for our in-sample period. This standardization limits the heterogeneity across the samples. The relative proportion of OTM calls and puts is stable, but we observe a nontrivial shift from ATM to deep OTM put options, with the former now representing about 32.5% and the latter 27% of the overall observations. To the extent that variation in the pricing of deep OTM put option prices is harder to accommodate than for ATM prices, this composition effect, all else equal, will imply a worse out-of-sample fit than would otherwise be observed.

2.2. The option surface characteristics

The option IV surface displays highly persistent and nonlinear dynamics that are difficult to convey effectively through a few summary measures. We provide a couple of alternative depictions that highlight different aspects of the dynamics. The first approach emphasizes the evolution of separate option surface characteristics. The second approach consists of a standard principal components analysis of the IV surface.

The option characteristics are plotted in Fig. 1. Level captures the average IV for ATM short-dated options, term structure reflects the difference between the IV of long and short maturity ATM options, skew measures the IV gap between short-dated OTM put and OTM call options, and skew term structure is the difference between the skew computed from long- and short-dated options. Definitions are in the caption to Fig. 1. Note, in particular, that we define the short- and long-term skew symmetrically with

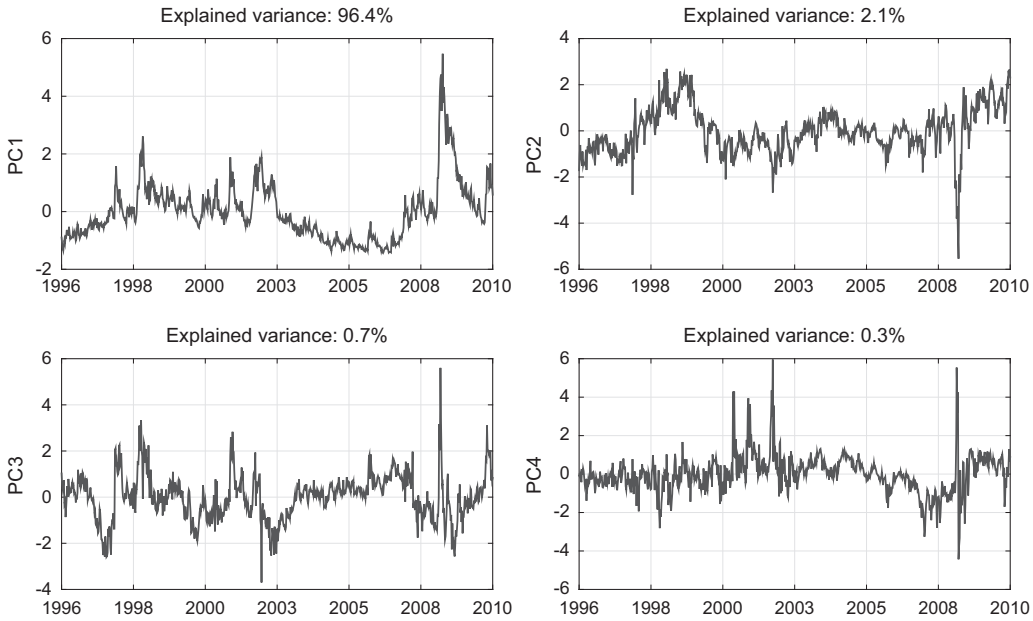

Fig. 1. Implied volatility (IV) surface characteristics. For Panel A, the IV level is the average IV for short at-the-money (ATM) options. For Panel B, the IV term structure is the difference in IV between long- and short-dated ATM options. For Panel C, the IV skew is the difference between the IV of short-dated out-of-the-money (OTM) put and OTM call options. For Panel D, the skew term structure is the difference between the long- and short-dated skew, with the long skew defined analogously to the short skew. Short-dated options are those with 0.1 years to maturity, and long-dated options have 0.8 year to maturity. ATM options have volatility-adjusted moneyness m equal to zero, OTM put options have $m=-2$, and OTM call options have $m=2$. Panel A: Implied volatility level, Panel B: Implied volatility term structure, Panel C: Implied volatility skew, Panel D: Implied volatility skew term structure.

Table 2
Summary statistics and correlation matrix for option characteristics.
The statistics for the implied volatility level, term structure (TS), skew, and skew term structure are computed over the in-sample period, January 1996 to July 2010.

Option	Summary statistics			Correlation matrix			
characteristic	Mean	Median	Standard deviation	Level	TS	Skew	Skew TS
Level	0.19	0.18	0.08	1.00	−0.69	0.89	−0.24
TS	0.01	0.02	0.03	–	1.00	−0.57	0.69
Skew	0.10	0.09	0.05	–	–	1.00	−0.31
Skew TS	0.04	0.04	0.03	–	–	–	1.00

respect to the degree of volatility-adjusted moneyness for the left and right tail, as advocated by Bates (1991).

The IV level displays not only occasional erratic spikes to the upside, but also strong persistence, as expected for a series reflecting the general level of volatility. Inspecting the remaining three panels, we notice a considerable degree of commonality. Every major spike in the IV level is visible in the other characteristics.

Table 2 supplements Fig. 1 with summary statistics for the IV surface characteristics. The correlation matrix confirms the strong covariation between the IV level and the remaining features. Moving to the other characteristics, the IV term structure is moderately positive, apart from episodic large negative outliers. The skew is consistently positive, exceeding 5% over the vast majority of the sample and averaging 10%. The skew also displays pronounced persistence and is particularly elevated when markets are turbulent. Finally, the skew term structure is mostly positive but spikes downward during steep market declines, indicating a dramatic flattening of the smirk at the onset of market crises. This feature accounts for a great deal of variation in the surface, as the skew is negatively correlated with the skew term structure. When the skew steepens drastically, the effect is much less pronounced at longer maturities. Hence, this type of excitement of the short left part of the IV surface must be associated with shocks to volatility and jump intensities of moderate persistence.

While a clear dependence exists between the option characteristics, both Fig. 1 and Table 2 suggest that the dynamics of the IV level cannot account for the overall surface dynamics. For example, the 1997 and 1998 crises have a much more pronounced and persistent effect on the skew than the IV level. Likewise, the aftermath of the 1998 Russian crisis is associated with a historically high upward-sloping term structure, and the IV level is close to its historical mean. In contrast, other periods with similar IV levels feature much flatter IV term structures.

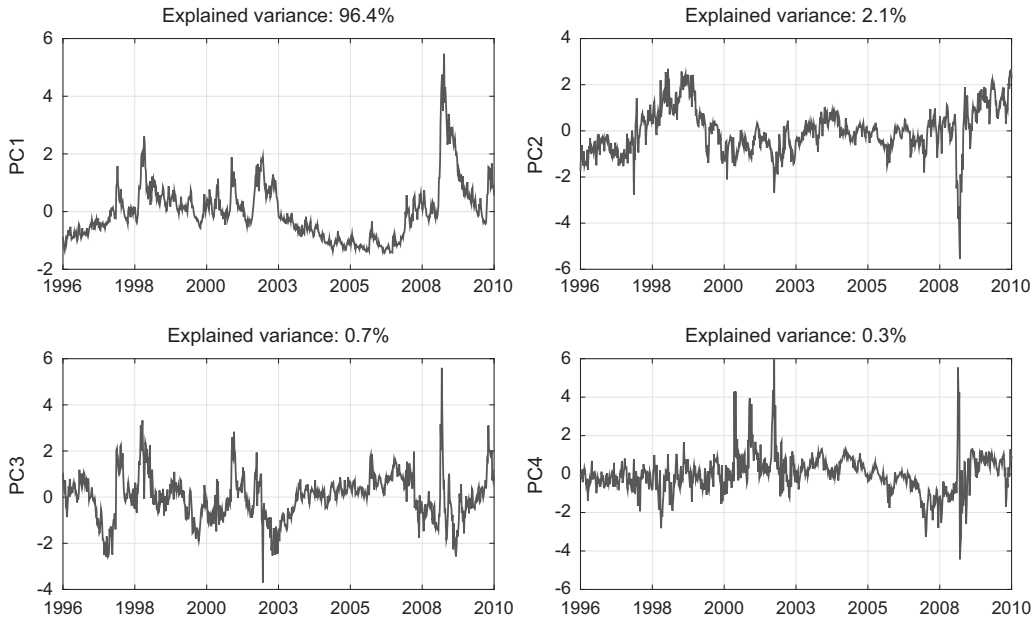

Fig. 2. Principal components (PCs) of the implied volatility surface. The graphs depict the first four principal components extracted from the Standard & Poor's 500 IV surface from January 1996 to July 2010. On each day we interpolate the IV surface to generate standardized options with the same volatility-adjusted moneyness, m, and tenor across the sample. We obtain option prices for m in the set $\{-4, -3, -2, -1, -0, 1, 2\}$ and tenor equal to three values, $\{0.1, 0.3, 0.8\}$ (in years). This produces a total of 21 synthesized option contracts per day. For each graph, we also report the percentage of the overall variation explained by the given principal component.

Table 3
Relating option characteristics and principal components (PCs).

We report the coefficients with t-statistics (in parentheses) and the R^2 from the linear regression of different options characteristics [level, term structure (TS), slope, and slope term structure] on the first four principal components extracted from the Standard & Poor's 500 implied volatility surface from January 1996 to July 2010. We also report the first sample autocorrelation coefficient and the average sample autocorrelation coefficient (AC) over two-to-ten and 11-to-20 lags of the regression residuals.

PC	Level	TS	Skew	Skew TS
PC1	0.19 (343.79)	−0.04 (−60.84)	0.11 (133.05)	−0.01 (−6.42)
PC2	−0.24 (−63.65)	0.40 (87.14)	−0.05 (−9.19)	0.41 (41.04)
PC3	−0.14 (−21.49)	−0.08 (−10.48)	0.45 (43.81)	−0.21 (−11.82)
PC4	−0.05 (−5.07)	−0.08 (−6.88)	−0.36 (−23.36)	0.03 (1.06)
R^2	0.99	0.94	0.96	0.71
AC(1)	0.66	0.60	0.32	0.44
AC(2:10)	0.39	0.26	0.21	0.26
AC(11:20)	0.27	0.16	0.12	0.16

Hence, we need a multifactor model to capture the dynamic dependencies between the option surface characteristics, as also concluded in Christoffersen, Heston, and Jacobs (2009).

Turning to the principal component (PC) analysis, Fig. 2 depicts the in-sample realizations of the first four PCs of the IV surface. It is evident that the first PC is closely related to the IV level and the second PC displays commonality with the IV term structure. However, the last two PCs appear largely unrelated to the characteristics depicted in Fig. 1. The first PC captures about 96.4% of the total variation, and the following PCs account for, respectively, 2.1%, 0.7%, and 0.3%. Clearly, there is a dominant level type effect, but this factor also accounts for a great deal of variation in the skew, term structure, and skew term structure, leaving, relatively speaking, only minor residual variation to explain for the remaining PCs.

To further explore how the PCs interact with the IV surface characteristics, Table 3 reports on the in-sample regression of characteristics on PCs. The table confirms the strong association of the first PC with the IV level, featuring a t-statistic beyond 300. For this PC, we also obtain the negative association with the IV and skew term structures and positive relation with the skew, matching the correlation patterns for the IV level in Table 2. In addition, we find the second PC to be associated with the IV term structure, corroborating the visual impression from Fig. 2. The third PC is associated with the skew as well as the skew term structure and level. However, the skew is much more strongly associated with the first PC so, effectively, the third PC

captures only residual skew variation that is largely orthogonal to the level. Finally, the fourth PC has no clear association with any of the characteristics. The variation in the skew term structure is effectively accounted for through the first two or three PCs.

These observations have a number of implications. First, no simple mapping exists between PCs and characteristics. Characteristics are intrinsically interconnected and covary strongly, so factors associated with the PCs generally exert a significant joint impact on multiple characteristics. Second, the difficulty of separating the forces driving the individual characteristics is a general feature of systems with pronounced nonlinearities. We see further evidence of potential nonlinearity in the strong serial correlation in the residuals of the regressions in Table 3. The first order autocorrelation coefficient is very large across all the characteristics and die out extremely slowly, suggesting highly persistent deviations from the linear approximation associated with the regression analysis. Third, the persistent residuals can be due to missing factors, and we find standard tests for the number of factors, see, e.g., Bai and Ng (2002), to indicate seven to eight factors. However, given the nonlinear association between option IV and (latent) factors, this likely reflects the failure of the linear approximation rather than the true number of underlying (linear) factors.[2]

In summary, accounting for a given model's ability to track the IV surface dynamics provides an intuitive way to highlight the implications of model misspecification. We later illustrate the quality of fit by comparing the model-implied and observed IV surface characteristics. No direct association exists between the inability to fit the dynamics of a specific set of characteristics and the lack of a given factor, because the factors' impact on the option IVs is highly nonlinear and creates correlated dynamic interactions across the characteristics.

3. Parametric modeling of the option panel

We turn next to parametric modeling of the options with the goal of succinctly capturing the IV surface dynamics via a low-dimensional state vector. We adopt a general-to-specific approach. The proposed model subsequently serves as the basis for our analysis of the equity and variance risk premia. The initial decision concerns the number of latent state variables to include. The vast majority of empirical option pricing studies employs a single stochastic volatility factor, but the literature on estimating the return dynamics under the physical measure and a few option pricing studies, e.g., Bates (2000), Christoffersen, Heston, and Jacobs (2009) , Christoffersen, Jacobs, and Ornthanalai (2012), and Andersen, Fusari, and Todorov (2015), point to a minimum of two factors. This is also consistent with our descriptive analysis of the IV surface in Section 2. Hence, we follow Andersen, Fusari, and Todorov (2015) in proposing a general three-factor model that, apart from the specification of the jump distribution, embeds most existing continuous-time models in the literature as special cases. We show that exponentially distributed price jumps provide a superior fit relative to the more commonly adopted Gaussian specification, justifying the alternative representation in our benchmark model.

Our three-factor model for the risk-neutral equity index dynamics is given by the following extension of the representation in Andersen, Fusari, and Todorov (2015):

$$\begin{aligned}
\frac{dX_t}{X_{t-}} &= (r_t-\delta_t)\,dt+\sqrt{V_{1,t}}\,dW^{\mathbb{Q}}_{1,t}+\sqrt{V_{2,t}}\,dW^{\mathbb{Q}}_{2,t}+\eta\sqrt{U_t}\,dW^{\mathbb{Q}}_{3,t}\\
&\quad+\int_{\mathbb{R}^2}(e^x-1)\tilde{\mu}^{\mathbb{Q}}(dt,dx,dy),\\
dV_{1,t} &= \kappa_1(\overline{v}_1-V_{1,t})\,dt+\sigma_1\sqrt{V_{1,t}}\,dB^{\mathbb{Q}}_{1,t}\\
&\quad+\mu_1\int_{\mathbb{R}^2}x^2 1_{\{x<0\}}\mu(dt,dx,dy),\\
dV_{2,t} &= \kappa_2(\overline{v}_2-V_{2,t})\,dt+\sigma_2\sqrt{V_{2,t}}\,dB^{\mathbb{Q}}_{2,t},\\
dU_t &= -\kappa_u U_t\,dt+\mu_u\int_{\mathbb{R}^2}\left[(1-\rho_u)x^2 1_{\{x<0\}}+\rho_u y^2\right]\mu(dt,dx,dy),
\end{aligned} \tag{3}$$

where $(W^{\mathbb{Q}}_{1,t}, W^{\mathbb{Q}}_{2,t}, W^{\mathbb{Q}}_{3,t}, B^{\mathbb{Q}}_{1,t}, B^{\mathbb{Q}}_{2,t})$ is a five-dimensional Brownian motion with $\text{corr}\left(W^{\mathbb{Q}}_{1,t}, B^{\mathbb{Q}}_{1,t}\right)=\rho_1$ and $\text{corr}\left(W^{\mathbb{Q}}_{2,t}, B^{\mathbb{Q}}_{2,t}\right)=\rho_2$, and the remaining Brownian motions are mutually independent. In addition, μ is an integer-valued measure counting the jumps in the price, X, and the state vector, (V_1, V_2, U). The corresponding (instantaneous) jump intensity, under the risk-neutral measure, is $dt\otimes\nu^{\mathbb{Q}}_t(dx,dy)$. The difference $\tilde{\mu}^{\mathbb{Q}}(dt,dx,dy)=\mu(dt,dx,dy)-dt\nu^{\mathbb{Q}}_t(dx,dy)$ constitutes the associated martingale jump measure.

The jump specification involves two separate components, x and y. The former captures co-jumps that occur simultaneously in the price, the first volatility factor, V_1, and, potentially, in the U factor (if $\rho_u<1$), and the latter represents independent shocks to the U factor.[3] The compensator characterizes the conditional jump distribution and is given by

$$\frac{\nu^{\mathbb{Q}}_t(dx,dy)}{dx\,dy}=\begin{cases}\left(c^-(t)\cdot 1_{\{x<0\}}\lambda_- e^{-\lambda_-|x|}+c^+(t)\cdot 1_{\{x>0\}}\lambda_+ e^{-\lambda_+ x}\right) & \text{if } y=0,\\ c^-(t)\lambda_- e^{-\lambda_-|y|} & \text{if } x=0 \text{ and } y<0.\end{cases} \tag{4}$$

The first term on the right-hand side, referring to the $x\neq 0, y=0$ case, reflects co-jumps in price and volatility, and the second term, $x=0, y<0$, captures independent shocks to the U factor. The individual (strictly positive)

[2] For a simple illustration, we calibrate a one-factor Heston model and derive the sensitivity of the IV surface to the volatility factor. For a given location in the surface, i.e., a given mildly OTM option, the sensitivity (derivative of the option IV with respect to volatility) typically varies dramatically with the level of volatility. Thus, strongly correlated approximation errors arise from linearizing the dependence of the surface characteristics to factors, as the true sensitivities fluctuate strongly over time. This illustration is provided in our Supplementary Appendix.

[3] The latter can also generate a jump in return volatility if $\eta>0$.

jumps in U are either independent from V_1 or proportional to the (simultaneous) jump in V_1. Following Kou (2002), we model the price jumps as exponentially distributed, with separate tail decay parameters, λ_- and λ_+, for negative and positive jumps. Moreover, for parsimony, the independent shocks to the U factor are distributed identically to the negative price jumps. Finally, the time-varying jump intensities are governed by the $c^-(t)$ and $c^+(t)$ coefficients. These coefficients evolve as affine functions of the state vector

$$c^-(t) = c_0^- + c_1^- V_{1,t-} + c_2^- V_{2,t-} + U_{t-}, \quad c^+(t) = c_0^+ + c_1^+ V_{1,t-} + c_2^+ V_{2,t-} + c_u^+ U_{t-}. \tag{5}$$

This representation involves a large set of parameters that can be hard to identify separately. At the estimation stage, we eliminate those that are insignificant and have no discernible impact on model fit. However, generality along this dimension is important, as the jump specification turns out to be critical for a suitable representation of the IV surface dynamics. For identification purposes, we set the coefficient in front of U in $c^-(t)$ to unity and, hence, the value of U directly signifies its contribution to the negative jump intensity.[4]

Our three-factor model possesses a number of distinctive features. The factors (V_1, V_2, U) drive both the diffusive volatility and the jump intensities. V_1 and V_2 are always present in the diffusive volatility, as in traditional multifactor volatility models, and U contributes to diffusive volatility only if $\eta > 0$. In fact, the constrained model arising for $\eta = 0$ is of separate interest. It implies that the factor U affects only the jump intensities, with no impact on diffusive volatility. Furthermore, in an extension to existing option pricing models, we allow positive and negative jump intensities to have different loadings on the latent factors. Some factors affect only positive or only negative jump intensities. Such flexibility in modeling the jump intensities is important given the nonparametric evidence in Bollerslev and Todorov (2011).

The jump modeling also involves several novel features. First, the price jumps are exponentially distributed. This is unlike most earlier studies, which rely on Gaussian price jumps, following Merton (1976).[5] Next, the jumps in the factor V_1 are linked deterministically to the price jumps, with squared price jumps impacting the volatility dynamics in a manner reminiscent of discrete GARCH (generalized autoregressive conditional heteroskedasticity) models.[6] For parsimony and ease of identification, we allow only the negative price jumps to impact the volatility dynamics. Finally, U is driven in part by the squared negative price jumps and in part by independent jumps, with the parameter ρ_u controlling the contribution of each component in the dynamics of U. As such, the model accommodates both perfect dependence ($\rho_u = 0$) and full independence ($\rho_u = 1$) between the jump risks of V_1 and U. Moreover, these state variables, governing critical features of the option surface dynamics, are related through the time variation in the jump intensity. Our specification allows for cross-excitation in which jumps in V_1 enhance the probability of future jumps in U, and vice versa.[7]

Differences in the jump distributions aside, our model nests most existing models. For the one-factor setting, with V_2 and U absent, we recover the double-jump volatility model of Duffie, Pan, and Singleton (2000), estimated using options data by Broadie, Chernov, and Johannes (2007). In the two-factor setting, with U absent and excluding volatility jumps, we obtain the Bates (2000) jump diffusion, and further ruling out price jumps leads to the two-factor diffusive model of Christoffersen, Heston, and Jacobs (2009). The key difference in our model from existing work is the separation of the left jump intensity from the volatility (and its components) and the right jump intensity (through the U factor).

We know of only two prior instances in which this type of separation is contemplated. Santa-Clara and Yan (2010) model jump intensity by a separate diffusive factor that can be correlated with volatility, which itself follows a diffusion. Hence, the model does not include volatility jumps, critical for fitting the option surface, as noted by Broadie, Chernov, and Johannes (2007) and further confirmed here. Christoffersen, Jacobs, and Ornthanalai (2012) consider a discrete-time GARCH model with conditionally Gaussian and non-Gaussian innovations (jumps of Merton type) in which conditional volatility and jump intensity are driven by past squared innovations. This model does not allow for closed-form solutions for the option prices, complicating inference from the option surface. Our model differs from these two papers along several dimensions crucial for the analysis of risk premia. First, we model only the risk-neutral distribution and do not assume any structure under $\mathbb{P}$. Thus, we do not import information from the physical return dynamics (other than no-arbitrage restrictions). This is critical for our subsequent findings regarding the drivers of risks and risk premia in Section 7. Second, we separate the dynamics of the left and

[4] The formal inference in Andersen, Fusari, and Todorov (2015) provides strong evidence for the presence of a separately evolving left jump tail factor like U in the risk-neutral return dynamics, while it is unclear if U also directly impacts spot volatility. As such, we let U enter the left jump intensity with a unitary coefficient. This resolves identification issues that arise regarding the scale of U versus the loading coefficient for U in the jump intensity. It is analogous to the imposition of a unitary coefficient for the volatility components in the return dynamics in Eq. (3).

[5] Bates (2012) studies the option pricing implications of models with exponential and Gaussian jumps. He finds them to be broadly similar for short-maturity options that are not deep OTM.

[6] Our modeling of the volatility jumps, and their dependence with the price jumps, deviates from earlier empirical option pricing studies, e.g., Duffie, Pan, and Singleton (2000), who model volatility jumps as exponentially distributed. In our case, they are the squares of exponentially distributed random variables and, hence, much fatter tailed. This

(*footnote continued*)
enhances the reaction of volatility to large price shocks. Finally, our modeling implies a nonlinear deterministic link between price and volatility jumps, unlike Duffie, Pan, and Singleton (2000). There is overwhelming empirical support for GARCH-like dynamics in volatility, similar to the continuous-time specification adopted here.

[7] We stress that the model, Eq. (3), still belongs to the affine family covered by Duffie, Filipović, and Schachermayer (2003) and, as shown in Andersen, Fusari, and Todorov (2015), the following parameter constraints ensure covariance stationarity of the latent factors:

$$\kappa_1 > \frac{2c_1^-\mu_1}{\lambda_-^2}, \quad \kappa_u > \frac{2\kappa_1\mu_u}{\kappa_1\lambda_-^2 - 2c_1^-\mu_1}, \quad \kappa_2 < 0, \quad \text{and} \quad \sigma_i^2 \le 2\kappa_i\bar{v}_i, \ i = 1, 2.$$

right jump intensities, which is important for the pricing of short maturity OTM puts and calls. Third, we adopt the double-exponential return jump distribution, providing a superior fit to the short maturity OTM options. Fourth, our specification involves cross-excitation in the jump and volatility dynamics, leading to improved characterization of longer maturity options, particularly in the aftermath of volatile episodes in the sample.

In summary, the main departure from prior work stems from the inclusion of the new U factor. Given the rather unconventional representation, we briefly discuss how this factor enhances the features of the risk-neutral dynamics. It is best seen by focusing on a restricted model in which we eliminate U from the diffusive volatility, i.e., set $\eta=0$, and further let $\rho_u=0$, so that there is no independent jump component driving U. In this scenario, there is no distinct source of risk impacting U. It is driven solely by the squared negative price jumps. Nonetheless, U affects the jump intensities and, hence, the option surface, separately from V_1. That is, to convey the current state of the system, U must be included among the components of the state vector.[8] In other words, even if the source of risk in U is spanned by the jumps in X and V_1, U is still necessary for characterizing the conditional risk-neutral distribution of future log returns or predicting the future evolution of the factors, even after controlling for the current values of V_1 and V_2. The role of U only expands, if it is subject to independent shocks as well. Below, we detail how the U factor impacts the IV surface characteristics over time.

The model in Eq. (3) pertains to the risk-neutral dynamics of X. However, due to the equivalence of $\mathbb{Q}$ and $\mathbb{P}$, the assumed dynamics have implications for the dynamics of X under $\mathbb{P}$ as well. In general, these implications are limited to those features of model (3), which hold almost surely. They consist of the following. First, the spot diffusive variance is invariant to the change of measure. In the model, this is given by

$$V_t = V_{1,t}+V_{2,t}+\eta^2 U_t. \tag{6}$$

Second, regarding the jumps, the only property that applies almost surely is the identity of the realized jumps in the returns and state variables. In particular,

$$\Delta V_{1,t} = \mu_1(\Delta\log(X))^2 1_{\{\Delta\log(X)<0\}}, \tag{7}$$

and, if $\rho_u=0$, we also have

$$\Delta U_t = (\Delta\log(X))^2 1_{\{\Delta\log(X)<0\}}, \tag{8}$$

under both measures.

In most empirical option pricing applications, additional assumptions are invoked when changing measure from $\mathbb{P}$ to $\mathbb{Q}$. For example, it is commonly assumed that the model class is identical, and affine, under both measures. This is convenient as affine models offer a great deal of tractability. However, this approach severely restricts the dynamics of the risk premiums. In addition, such structure preserving transformations (SPTs) impose auxiliary restrictions, extending to the model parameters. In our affine setting, the SPT assumption implies that $\sigma_1, \sigma_2, \eta, \rho_1, \rho_2, \rho_u, \mu_1$, and κ_3 are identical under $\mathbb{P}$ and $\mathbb{Q}$, and the remaining parameters could differ.

Data on the underlying equity-index values can be helpful in the estimation of the risk-neutral model. Below, we impose the pathwise (almost sure) restriction regarding the spot variance in estimation. Given the difficulty in recovering spot volatility jumps from high-frequency data, due to both estimation uncertainty and lack of overnight observations, we do not impose restrictions regarding the pathwise (realized) price and volatility jump relation implied by our risk-neutral model. Finally, if one constrains the pricing of risk through a SPT from $\mathbb{P}$ to $\mathbb{Q}$, additional information from the $\mathbb{P}$ dynamics can be imported from the underlying return data during estimation of the risk-neutral dynamics. This comes, however, with the risk of severe model misspecification. The option panel is very informative about the risk-neutral dynamics, so we avoid auxiliary restrictions that can induce model misspecification with unpredictable impact on our inference for the risk premia.

4. Estimation

This section first introduces our estimation approach and then presents estimation results.

4.1. Estimation approach

The development of formal tools for parametric inference in the context of an option panel is challenging. There are pronounced time series dependencies in the latent volatility components, and, potentially, the jump intensities. At the same time, sizable bid–ask spreads influence the observed prices and quotes for the options. These measurement errors are strongly heterogeneous and correlated with the overall return variation. Finally, no-arbitrage constraints at any time link the individual option prices across strikes and they equate the spot diffusive volatility for the underlying asset (imperfectly observable from high-frequency returns) with the volatility implied by the contemporaneous state vector (also extracted with a degree of statistical error) for every option cross section. Consequently, we adapt the parametric estimation and inference approach put forth in Andersen, Fusari, and Todorov (2015) that is designed to deal with this type of environment. It exploits in-fill asymptotics in the option cross section: i.e., it operates under the assumption that, for a small set of maturities that can vary from day to day, option prices are observed across a broad range of strikes with only small gaps between the exercise prices.

The approach provides consistent period-by-period estimates for the state vector along with valid asymptotic inference for the state vector and model parameters as well as the fit to specific regions of the IV surface on any given day. This is possible due only to the adoption of the

[8] This is a reflection of the fact that no direct association exists between the dimensionality of the sources of risk and the dimension of the state vector required to characterize the conditional dynamics of the system. This phenomenon arises naturally in continuous-time autoregressive-moving average (ARMA) models, see, e.g., Brockwell (2001). It is also a well-known feature of the so-called quadratic term structure models, see, e.g. Ahn, Dittmar, and Gallant (2002) and Leippold and Wu (2002).

in-fill asymptotic scheme for the option cross section.[9] In practice, this reflects the actual structure of our panel. The option quotes are clustered closely in the strike range, and we use only weekly observations of the option cross section. Thus, the well-recognized advantages of inference via high-frequency data apply naturally to the cross section, not the time series, in our setting.

The wealth of information embedded in the option cross section is well recognized. It is known to facilitate nonparametric extraction of the conditional risk-neutral density for the underlying asset returns across the maturities available on a given day. Through the imposition of a general parametric structure and inference procedure, we let the dynamic evolution of the conditional densities speak to the number of factors and to the intertemporal variation in volatility and jump intensities. Given the identified factors and model parameters, the individual cross section identifies the current state vector. In theory, the entire system can be identified and estimated consistently from a single cross section. However, the identification from a single option surface is weak. The use of a large number of surfaces, i.e., an option panel, allows the variation in the state vector over time to assist in identifying the underlying structure governing the option prices and helps diversify the idiosyncratic measurement errors.[10]

We denote the parameter vector of model (3) by θ and the state vector at time t by $\mathbf{Z}_t = (V_{1,t}\ V_{2,t}\ U_t)$. Further, the model-implied Black-Scholes IV is given by $\kappa(k,\tau,\mathbf{Z}_t,\theta)$ and the model-implied diffusive spot variance by $V(\mathbf{Z}_t,\theta) = V_{1,t}+V_{2,t}+\eta^2 U_t$. Letting n denote the (equidistant) frequency by which we sample the high-frequency asset returns, our estimator takes the form

$$\left(\{\widehat{V}^n_{1,t},\widehat{V}^n_{2,t},\widehat{U}^n_t\}_{t=1,\ldots,T},\widehat{\theta}^n\right) = \underset{\{\mathbf{Z}_t\}_{t=1,\ldots,T},\theta\in\Theta}{\arg\min} \sum_{t=1}^{T}\left\{\frac{\text{Option Fit}_t+\lambda\times\text{Vol Fit}_t}{V_t^{ATM}}\right\},$$

$$\text{Option Fit}_t = \frac{1}{N_t}\sum_{j=1}^{N_t}\left(\overline{\kappa}_{t,k_j,\tau_j}-\kappa(k_j,\tau_j,\mathbf{Z}_t,\theta)\right)^2,$$

$$\text{Vol Fit}_t = \left(\sqrt{\widehat{V}_t^{(n,m_n)}}-\sqrt{V(\mathbf{Z}_t,\theta)}\right)^2, \tag{9}$$

where $\widehat{V}_t^{(n,m_n)}$ is a nonparametric estimator of the diffusive spot variance constructed from the underlying intraday asset prices, as detailed in the Appendix, and V_t^{ATM} is the squared short-term ATM Black-Scholes IV.[11] Finally, λ is a tuning parameter, which we set to 0.2.[12]

The estimator (9) minimizes the weighted mean squared error in fitting the panel of observed option IVs, with a penalization term that reflects the deviation of the model-implied spot variance from a model-free spot variance estimate. The presence of the volatility fit in the objective function not only facilitates the incorporation (statistically) of the no-arbitrage constraint, but also serves as a regularization device for the estimation by penalizing parameter values that imply unreasonable volatility levels. Moreover, the standardization by V_t^{ATM} implies that we weigh observations on high and low volatility days differently. This improves efficiency as the measurement errors in the option prices and the estimation errors for the state vector generally rise with market volatility.[13]

The estimator (9) is derived via joint optimization over parameters and state vector realizations. This high-dimensional problem is tractable due to the particular form of our objective function: The terms corresponding to a given observation time depend on the state vector only through the option prices and nonparametric spot volatility estimate for that particular day. Thus, given a candidate θ vector, we trivially obtain the corresponding state vector realization. Hence, we concentrate, or profile, the state vector and optimize over the model parameters via Markov Chain Monte Carlo-based estimation, using a chain of length ten thousand, following Chernozhukov and Hong (2004).

4.2. Estimation results

As noted in Section 3, we follow a general-to-specific approach to estimation. Consequently, model (3) is very richly parameterized, particularly regarding the specification of the jump intensities. The idea is to allow for full generality and then eliminate the insignificant features in the model. For brevity, we defer the estimation results for the general case to the Supplementary Appendix. It turns out that the jump-loading parameters, c_0^-, c_2^-, c_u^+, are statistically insignificant, and the same applies for η. Hence, our more parsimonious model constrains these parameters to zero. For the negative jump intensity coefficients, this is readily interpreted. It implies that the frequency of jumps is governed exclusively by the level of the two factors, V_1 and U. The $\eta = 0$ and $c_u^+ = 0$ restrictions are more fundamental. First, $\eta = 0$ implies that U is a pure jump intensity factor that does not contribute directly to the diffusive volatility. This represents a major departure from existing continuous-time models, which are built from stochastic volatility factors.[14] Second, the elimination of c_u^+ means that U is constrained to affect only the negative jumps. Again, this is an important departure from existing asset pricing models. These features are precluded in the typical approach to empirical option pricing, because this approach is built around multifactor volatility

[9] Alternative inference techniques can generate unbiased estimates for the state vector realizations, determining the values of the volatility components and jump intensities, but cannot achieve consistency, thus rendering formal inference regarding the state vector and IV surface fit on a period-by-period basis infeasible.

[10] However, one year of option data, along with the high-frequency returns used to enforce the (statistical) equality of spot volatility across the $\mathbb{P}$ to $\mathbb{Q}$ measures, usually suffices for reasonable identification.

[11] This measure is obtained for the shortest available maturity on day t and for the option closest to at-the-money, with the associated forward rate deduced from put-call parity.

[12] In general, given the noise in the high-frequency spot volatility estimate, we should pick a relatively low value for λ. In the Supplementary Appendix, we report further evidence corresponding to different values of λ.

[13] Our specific weighting scheme stems from an analysis of the option pricing errors, showing that their volatility is roughly linear in the level of market volatility.

[14] Instead, our specification shares critical features with the discrete-time GARCH-type model of Christoffersen, Jacobs, and Ornthanalai (2012).

models with a single (Gaussian) price jump component. These models rule out pure jump dynamic factors and do not allow for factors to impact the negative and positive jump intensities differentially. In our case, by letting the option panel determine the fit, we find the risk-neutral dynamics to involve a factor — unrelated to volatility — that operates only on the negative jump intensity.

The estimation results for the general model (3) further reveal that the parameters controlling the risk-neutral law of U are not estimated precisely. This result is largely due to the fact that the persistence of U is rather extreme with a half-life of approximately eight years. With such a low degree of mean-reversion, the parameters κ_u, μ_u, and ρ_u cannot be recovered precisely as they play an insignificant role in determining the values of options with maturities of up to one year. A precise estimation of κ_u, μ_u, and ρ_u requires far longer-dated options than available in our sample. This issue also arises in the analogous case of recovering the risk-neutral volatility parameters from options data if the volatility is very persistent; see, e.g., Broadie, Chernov, and Johannes (2007) and the references therein. Nonetheless, we have compelling evidence for the presence of U in the risk-neutral dynamics. First, the hypothesis that U is absent is a joint hypothesis that $\mu_u = 0$ and that the vector $\{U_t\}$ is not present, and such a hypothesis is strongly rejected by the data.[15] Second, a constrained model in which U is absent performs significantly worse, both in- and out-of-sample, as shown in the Supplementary Appendix. Finally, even though the individual parameters κ_u, μ_u, and ρ_u are poorly identified, the realizations of the tail factor U are well identified. As discussed previously, the tail factor is crucial for our analysis of the risk-premium dynamics, as U represents the component of the left tail dynamics that is not tied to volatility.

The case of ρ_u is particularly interesting as this parameter is not endowed with a natural boundary condition that eliminates an associated feature from the model. Instead, it indicates the relative jump size in U stemming from (squared) co-price jumps versus a separate source of jumps. As such, the parameter is restricted to the $[0, 1]$ interval, with the boundary values indicating either that U does not co-jump with the price process ($\rho_u = 0$) or that U is not subject to separate jump shocks ($\rho_u = 1$). Our estimation results suggest that ρ_u is sufficiently poorly identified that, at standard significance levels, we cannot rule out any value in $[0, 1]$. However, as we show below, ρ_u turns out to be largely irrelevant for the extracted state vector realization throughout the sample.[16] Thus, we constrain ρ_u to fall within the unit interval.

We now turn to the results for the restricted model obtained after zeroing out c_0^-, c_2^-, c_u^+, and η.[17] Table 4 reports the point estimates and associated standard errors. As expected, the volatility factors differ significantly in their degree of mean-reversion, with V_2 having a half life of about five months versus three weeks for V_1. V_2 is also generally larger and has a lower volatility-of-volatility coefficient than V_1, implying a smaller and rapidly moving volatility factor and a larger, less volatile, but more persistent second volatility factor. Both display a strong negative association with the return innovations, generating an overall correlation between return and spot volatility innovations of around -0.95.[18]

Turning to the left tail factor, we find U to have an estimated half-life of eight years under the risk-neutral measure, thus far exceeding those of the volatility factors. Hence, this pure jump factor has the potential to impact the option prices substantially across both short and long maturities. Comparing our results with option-based estimation of multifactor volatility models, reported in Bates (2000) and Christoffersen, Heston, and Jacobs (2009), we find that the mean-reversion of the volatility in our model is far stronger than reported in the above-mentioned papers. This is compensated by the presence of the very persistent U factor. In the traditional volatility models, the left and right jump intensities are proportional to the volatility factors. In our case, through the introduction of U, we drive a wedge between volatility and jump intensity, and the option data identify jump intensity as the more persistent one. Intuitively, because U controls the left jump tails, this result stems from the relative expensiveness of the OTM long maturity puts across our sample, i.e., the comparatively slow flattening out of the IV skew at long maturities.

5. Diagnostic of the option panel fit and model performance

In this section, we explore whether model (3) provides a satisfactory characterization of the option surface dynamics. For this purpose, we first consider a sequence of more standard specifications as competitor models. They range from an extended version of the one-factor double-jump model of Duffie, Pan, and Singleton (2000) to a model including three stochastic volatility factors. The one-factor model (1FGSJ) features square-root volatility and a correlation between Gaussian return and exponential volatility co-jumps, and it has a time-varying jump intensity given as an affine function of the volatility state. To allow additional flexibility, we consider the two-factor version of the double-jump (stochastic volatility) model, and we explore both a Gaussian (2FGSJ model) and a double-exponential (2FESJ model) jump distribution for the return jumps. Finally, we expand the most successful in-sample two-factor model into a three-factor return-volatility co-jump model (3FESJ-V) by introducing a third square-root volatility factor, thus expanding the number of factors in the traditional manner. The exact specifications for each of the alternative models and the corresponding in-

[15] More formally, under the null that $\mu_u = 0$, the factor realization $\{U_t\}$ as well as the parameters κ_u and ρ_u are not identified. Hence, testing such a hypothesis using a standard t-test (or Wald test) is invalid. See Andrews (2001).

[16] We verify that imposing $\rho_u = 0$ or $\rho_u = 1$ has no material impact on any of our qualitative conclusions.

[17] A standard Wald test for the four parameters jointly taking the value of zero generates a p-value of 27.25%, confirming that we cannot reject this restriction at any standard level of significance.

[18] The value of this correlation coefficient varies with the relative size of the two factors. The reported value is obtained for the spot variances equaling their unconditional time series means. In light of the reported standard errors, this strongly negative coefficient is consistent with recent evidence exploiting an entirely different approach based on joint high-frequency data for volatility indices and underlying asset returns. See, e.g., Andersen, Bondarenko, and Gonzalez-Perez (forthcoming).

Table 4
Estimation results.

Model (3) is estimated using Standard & Poor's 500 equity-index option data sampled every Wednesday over the period January 1996 to July 2010 and the parameters η, c_u^+, c_0^-, and c_2^- are all set to zero. Parameters are reported in annualized return units.

Parameter	Estimate	Standard deviation
ρ_1	−0.959	0.093
$\overline{v}_1$	0.003	0.000
κ_1	10.989	0.193
σ_1	0.249	0.028
μ_1	12.158	0.247
ρ_2	−0.979	0.033
$\overline{v}_2$	0.010	0.000
κ_2	1.864	0.103
σ_2	0.170	0.006
μ_u	7.124	24.096
κ_u	0.0877	0.123
ρ_u	0.513	4.404
c_0^+	0.372	0.029
c_1^-	111.061	4.446
c_1^+	25.855	4.971
c_2^+	81.719	6.947
λ_-	25.944	0.196
λ_+	36.620	0.857

sample parameter estimates and root-mean-square error (RMSE) fit to the option panel are provided in the Supplementary Appendix. Generally speaking, they represent more elaborate specifications than estimated in the literature and, thus, afford an improved in-sample fit to the option surface relative to many of the models considered in prior studies.

At this stage, we simply note that model (3) has a considerably lower overall RMSE to the option panel of 1.71% compared with RMSE values ranging from 3.14% for the one-factor Gaussian double-jump model to 1.86% for the three-factor return-volatility co-jump model.[19] Thus, model (3) provides a comparatively good fit to the surface. However, it is less evident whether this translates into an improved characterization of the key dynamic factors determining the evolution of, and associated risks related to, the IV surface and the corresponding risk premiums. To this end, in this section, we provide additional details concerning the model fit to the option characteristics and the fit to the nonparametric volatility estimates from high-frequency data. We conclude the section with various robustness checks.

5.1. State vector dynamics, volatility surface dynamics, and jump intensities

We first analyze the state vector in our model. Table 5 reports summary statistics for the extracted time series of the three factors. We find that the jump volatility factor, V_1, is the dominant component of the diffusive volatility under the physical probability measure, contributing roughly two-thirds to its total mean. The two volatility factors also exhibit some negative correlation (of order −0.3), and V_1 is only slightly less persistent than V_2 under the statistical measure. Next, the mean of U implies it contributes an average of 3.7 negative jumps per year to the negative jump intensity. Thus, given the average negative jump arrival of 5.6, U is the dominant driver of the negative jump tail. Moreover, the sample standard deviation of U indicates a substantial degree of variation over time, inducing significant fluctuations in the negative jump tail and the associated (high) price for market downside protection. In addition, we find that, under $\mathbb{P}$, U is, by far, the most persistent of the three state variables. Finally, U exhibits nontrivial positive correlation with V_1 and slight negative correlation with V_2. This is consistent with our risk-neutral model (3), in which V_1 and U are connected through the jumps and the feedback effect induced by the jump intensities of the two state variables.[20]

To gain further insight into the dynamics implied by the model estimates, in Fig. 3, we plot the model-implied spot diffusive volatility, given by $\sqrt{V_1+V_2}$, and the corresponding high-frequency nonparametric estimate in the upper panel, and the model-implied estimates of $\sqrt{U}$ are depicted in the lower panel. The plots are intriguing along several dimensions. First, the option-implied estimate of the diffusive volatility has approximately the same sample mean as the nonparametric high-frequency estimate, but it is far less noisy, illustrating the potential gains from incorporating option information into volatility inference. Second, spikes emerge in market volatility and, even more strikingly, in U around well-known crises. Third, the negative jump intensity factor U portrays a very different picture than the diffusive volatility. For example, the peaks of U in the 1997 and 1998 crises and the European sovereign debt crisis match or exceed those observed from 2000 through 2003, yet the model-implied volatility is substantially higher in the latter than the former episodes. That is, the alternating shapes of the option surface signal that these events represent very different types of exposure to volatility and negative jump risks. Fourth, as expected, the financial crisis stands out from the rest. Moreover, the jump intensity factor U mean-reverts much slower than volatility following this crisis. The identical pattern is observed across all the episodes identified above in which the jump intensity rises strongly relative to volatility. This implies that U contributes (relatively) more to the expensiveness of OTM puts in the aftermaths of the Asian, Russian, and European crises than market volatility. The opposite is true for the turbulent episodes surrounding the September 11, 2001 attacks and the Second Gulf War in 2002, when market volatility clearly is the dominant force. Likewise, the initial spike in the jump intensity during the financial crisis was not caused solely by the U factor. Instead, U is accountable for the subsequent slow mean-reversion. Fifth, even during the quiet period 2004–2006, the negative jump intensity factor U remains at a nontrivial level, implying approximately one jump per year.

[19] Using the asymptotic theory developed in Andersen, Fusari, and Todorov (2015), these differences in RMSE are highly statistically significant.

[20] However, Table 5 concerns the statistical measure, and model (3) characterizes the risk-neutral measure. In general, no-arbitrage does not restrict the relation between the moments under the two measures.

Table 5
Summary statistics for the recovered state vector.
AC denotes autocorrelation, and Q signifies quantile. Sample averages are for the period January 1996 to July 2010.

Factor	Mean	Standard deviation	Skew	Kurt	AC(1)	AC(15)	AC(30)	Q(0.25)	Q(0.50)	Q(0.75)
V_1	0.017	0.035	5.037	36.687	0.884	0.250	−0.006	0.0001	0.0053	0.0162
V_2	0.012	0.009	0.737	3.363	0.840	0.369	0.102	0.0052	0.0103	0.0180
U	3.710	3.347	1.861	7.372	0.973	0.591	0.360	1.2538	2.8982	4.9409

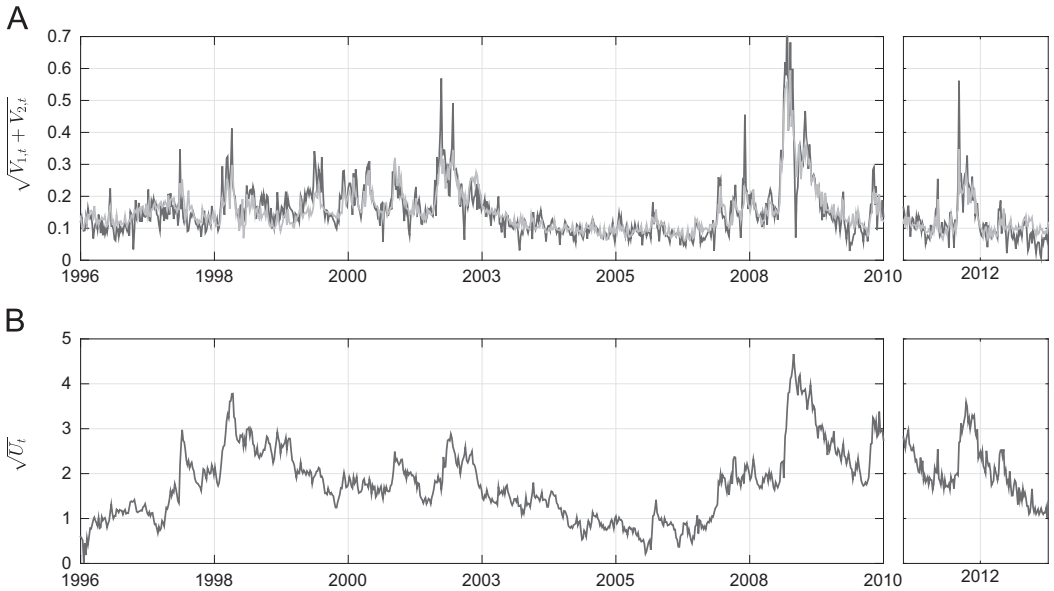

Fig. 3. Spot volatility and the U factor. Panel A displays the spot diffusive volatility estimated from the high-frequency data (the dark line) and from the option panel (the light-colored line). Panel B displays the estimate of $\sqrt{U}$. Panel A: Spot volatility, Panel B: U factor.

5.2. Fitting the option characteristics

Next we investigate the model's success in capturing the dynamics of the option panel. Recall from Section 2 that the first principal component of the option surface explains over 96% of the total variation, but the PCs fail to succinctly capture the dynamic dependencies of the option characteristics. The first principal component provides a fit (in RMSE) with the set of standardized options used in the PC analysis of 3.38%. We can compare this RMSE to the ones obtained by our parametric no-arbitrage models, reported in Table 6. Even, the simplest one-factor 1FGSJ model provides a significantly improved fit of 2.67% and this further drops to 1.40% for our preferred three-factor model. This is due to the nonlinear factor structure for the option panel implied by the parametric models (see footnote 2). For the remainder of this subsection, we analyze the success of the parametric models in tracking the dynamics of the IV surface by focusing on their ability to fit the option characteristics.

In Fig. 4 we plot the characteristics along with the model-implied fit. Perhaps not surprisingly, the model provides a near perfect fit to the IV level, for periods of both turmoil and relative tranquility. The fit to the IV skew is also satisfactory,

Table 6
Fit to options, characteristics, and spot volatility.
The numbers in the table are the root-mean-square errors (in percent) from fitting the implied volatility (IV) surface characteristics, the spot volatility, the implied volatilities for fixed moneyness $m \in \{-4, -3, -2, -1, -0, 1, 2\}$ and tenor $\tau \in \{0.1, 0.3, 0.8\}$, and all options used in the estimation. The models in the comparison are defined as follows. 1FGSJ (2FGSJ) refer to the one- (two-) factor Gaussian jump model with time-varying jump intensity; 2FESJ refers to the two-factor exponential jump model with time-varying jump intensity; 3FESJ-V refers to the three-factor exponential jump model with time-varying jump intensity; and 3F refers to the three-factor exponential jump model with the separate jump factor, U in Eq. (3). All models are explicitly defined in the Supplementary Appendix.

Option characteristic	Model fit				
	1FGSJ	2FGSJ	2FESJ	3FESJ-V	3F
IV level	1.73	1.01	0.88	0.68	0.64
IV term structure	2.72	1.42	1.06	1.30	0.86
IV skew	3.81	2.88	2.54	2.13	1.96
IV skew term structure	2.79	3.70	2.01	2.57	2.40
Spot volatility	5.199	4.130	3.944	3.945	3.977
Options with fixed m, τ	2.67	2.10	1.89	1.58	1.40
All options	3.14	2.56	2.07	1.86	1.71

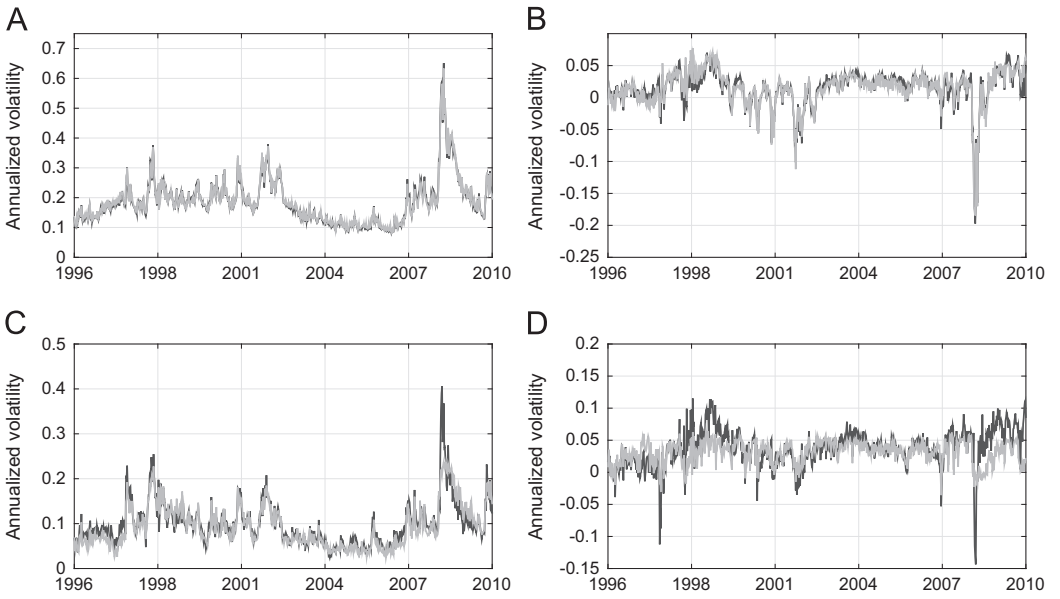

Fig. 4. The model-implied fit to the option characteristics. The dark line corresponds to the data, and the light-colored line refers to the fit by model (3). Panel A: Implied volatility level, Panel B: Implied volatility term structure, Panel C: Implied volatility skew, Panel D: Implied volatility skew term structure.

although the model slightly overestimates the skew during 1999 and tends to underestimate it at peaks of financial crises. Nonetheless, no evidence exists of major systematic biases and the relative errors are small except for the fall of 2008.[21] Turning to the IV term structure, we observe, from the top right panel of Fig. 4, that our model provides an almost perfect fit to this characteristic. Finally, the most challenging feature of the surface is the IV skew term structure. Nonetheless, the model fits this feature well except for two noticeable periods, namely, the aftermaths of the 1998 Russian crises and the recent financial crisis. During these episodes, our model predicts a somewhat steeper IV skew term structure than observed. Intuitively, this is indicative of negative jump tails that need to be even more persistent, during these two periods, than the model implies to deliver the slower thinning of the risk-neutral tails along the maturity dimension of the conditional return distribution.

To benchmark the success of model (3) in capturing the option surface characteristics, we now compare it with the fit provided by the alternative stochastic volatility models. The results are presented in Table 6. Our estimation does not minimize the distance between the observed and model-implied option characteristics. Nevertheless, our model provides a superior fit to each of the four option characteristics. The improvement is significant compared with one- and two-factor models with Gaussian price jumps. Moreover, the improved fit offered by our model is not solely attributable to the addition of an extra factor. The alternative three-factor model performs significantly worse at fitting the term structure of the IV level and skew. Furthermore, removing U (leading to the model 2FESJ) produces a significant deterioration in the fit to the IV skew. Finally, our model improves substantially on 1FGSJ and 2FGSJ models in fitting the spot volatility and is essentially on par with the rest of the alternative specifications in this regard.

The distinguishing feature of model (3) is the presence of U, which resides only in the negative risk-neutral jump intensity. We now explore the specific role of U in driving the surface dynamics. To this end, in Fig. 5, we plot the fitted IV surface characteristics and their sensitivity with respect to U at the current values of the state vector for each day in the sample. These sensitivities are measured via the change of the characteristics stemming from increases and decreases in U by 50% from its estimated value. For the IV level, U has a limited impact except for crises periods when volatility is very high. This is to be expected as short-term ATM IV is primarily determined by the level of the diffusive volatility (U is absent). Meanwhile, U has a very pronounced and more uniform impact on the IV skew. That is, the significance of U for the skew is ubiquitous and remains nontrivial, even during the tranquil period of 2004–2006. Turning to the IV term structure in Panel B of Fig. 5, we observe strong time variation in the impact of U, with the effect being most substantial following the Asian, Russian, and recent financial crises. In contrast, U has a very limited effect on the IV term structure during 2004–2006. This is not surprising. The intensity of the volatility jumps in model (3) depends on U. Hence, a higher value of U today triggers higher expected future diffusive volatility, and given the persistence of U under $\mathbb{Q}$, this effect is long-lasting and tends to elevate the

[21] Our finding of underestimation of the skew during highly turbulent periods is consistent with recent nonparametric evidence in Bollerslev and Todorov (2014) of time variation in the shape of the jump tails. Accounting for such a feature of the data alleviates the slight mispricing during such periods, observed in Fig. 1, but it takes us outside the tractable generalized affine framework. Some of the time variation in the shape of jump tails can be partially offset by very high values of the U factor, which is not constrained to be part of volatility. Furthermore, the measurement errors in the option prices during crises periods are exceptionally large, so gauging model quality by the size of the pricing errors during these periods is potentially misleading.

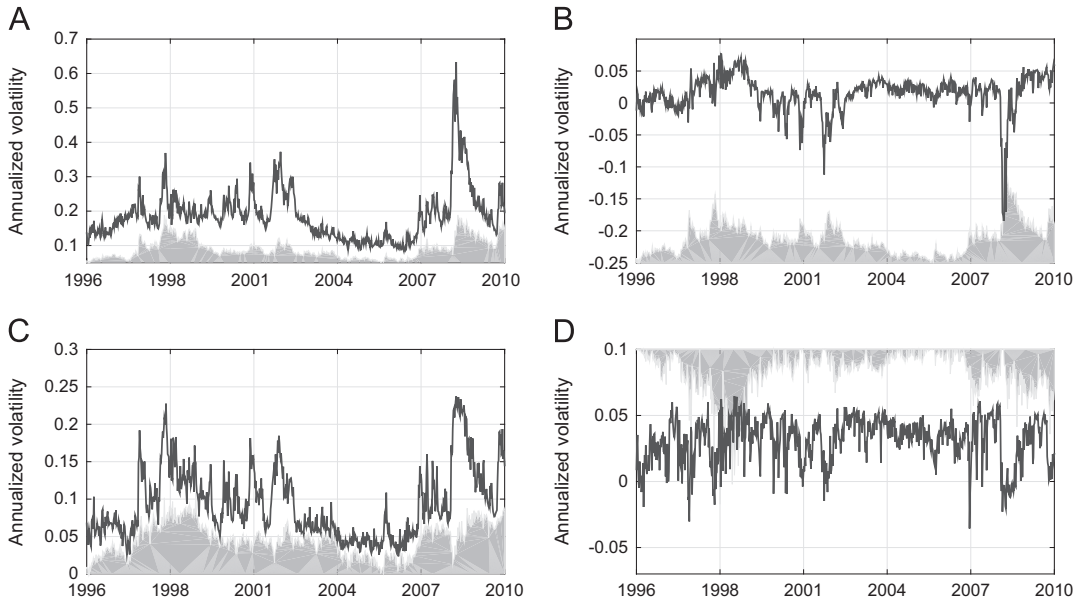

Fig. 5. The effect of U on the option characteristics. The line corresponds to the fitted characteristics, and the shaded area indicates the change in the characteristics stemming from a decrease versus an increase in U by 50% relative to the current estimated value. To better capture the effect of U on the option characteristics, we use only the days in the sample for which the shortest maturity of the options is less than ten business days in the computation of the shaded area. Panel A: Implied volatility level, Panel B: Implied volatility term structure, Panel C: Implied volatility skew, Panel D: Implied volatility skew term structure.

IV term structure following the crises of 1997, 1998, and 2008. Finally, U has a relatively small impact on the IV skew term structure, except when U is very high. Overall, Fig. 5 shows that U has a significant impact on both the term structure and the skew. The impact on the skew is largely immune to the state of the system, and the impact on the term structure is concentrated in extended periods following some of the crises in the sample. This effect of U on the surface helps account for the dynamic interdependencies among the characteristics discussed in Section 2.

5.3. Robustness of estimation results and inference

We next explore the robustness of our empirical findings. First, we check the sensitivity with respect to the penalization term for the volatility fit in the objective function. We vary λ around the original choice of 0.2 by 50% in either direction. It is useful when interpreting the results below to keep in mind that a misspecified model faces tension in simultaneously fitting the option surface and matching the high-frequency based estimate of spot volatility. The results are reported in the Supplementary Appendix. We note the remarkable stability of the parameters with the exception of σ_2 and c_0^+ for which the changes are somewhat large compared with the precision in their recovery. Hence, some evidence exists for misspecification, but the critical features of the system remain virtually unchanged. Most significant, the extracted tail factor U is unaffected, which is crucial for our analysis of the risk premium dynamics later on.

Second, the Supplementary Appendix reports results for subsample estimation covering 1996–2006 and 2007–2010. The fit is excellent for the longer 1996–2006 subsample, with an overall RMSE of 0.99%. While this sample excludes the financial crisis and, thus, poses less of a challenge to the option pricing model, the sample still covers some dramatic episodes around 1997, 1998, and the Internet bubble, along with some extremely low volatility levels during 2004–2006. The shorter and extremely turbulent 2007–2010 period is much harder to accommodate, and the RMSE is 2.16%. We do observe some degree of parameter instability, mainly impacting the risk-neutral means of the two volatility factors, $\overline{v}_1$ and $\overline{v_2}$, which tend to move in opposite directions, and the loadings on the volatility factors in the jump intensities. This is indicative of some misspecification in the modeling of diffusive volatility. Nonetheless, the parameters λ^- and λ^+, governing the jump tail decays, are remarkably stable across subsamples. Likewise, the estimates of μ_1, controlling the volatility jumps, are stable. And most important for our analysis, the extracted realization of U, across the entire sample, remain near invariant regardless of whether the full sample or subsample parameter estimates are employed.

6. Out-of-sample performance

Our model (3) is richly parameterized, containing three state variables along with the 18 separate parameters reported in Table 4. This could raise concerns regarding potential in-sample overfitting. We address this issue by exploring the out-of-sample performance vis-à-vis the more parsimoniously parameterized alternatives introduced in Section 5. If the dynamic features extracted from the option surface through model (3) are genuine and stable, the model should continue to provide a superior fit also for the options observed beyond the in-sample period.

To assess the robustness of model (3) relative to the alternative specifications, we use the parameters for each model estimated over the period January 1, 1996 to July 21,

Table 7
Out-of-sample option pricing performance and volatility fit.

We report root-mean-square errors (RMSEs) in implied volatility (in percent). The abbreviations for the different models are as in Table 6. RRMSE is the ratio of the RMSE of a given model over that of the 3F model minus one.

Panel A: Overall option RMSE

	1FGSJ	2FGSJ	2FESJ	3FESJ-V	3F
RMSE	3.28	2.66	2.25	2.26	1.77

Panel B: Sorting by moneyness and maturity

Moneyness	1FGSJ		2FGSJ		2FESJ		3FESJ-V		3F	
	RRMSE		RRMSE		RRMSE		RRMSE		RMSE	
τ	≤ 60	>60	≤ 60	>60	≤ 60	>60	≤ 60	>60	≤ 60	>60
$m \leq -3$	0.68	1.16	0.60	0.48	0.09	0.33	0.14	0.30	2.28	2.76
$m \in (-3,-1]$	0.49	0.71	0.32	0.34	0.14	0.33	0.03	0.47	1.53	1.95
$m \in (-1,1]$	1.43	0.39	0.99	0.30	0.74	0.08	0.67	0.16	0.91	1.36
$m > 1$	1.77	0.70	0.89	0.38	0.98	0.15	0.82	0.07	1.24	1.86

Panel C: Spot volatility RMSE

	1FGSJ	2FGSJ	2FESJ	3FESJ-V	3F
RMSE	6.23	5.01	4.05	4.27	3.82

2010 to price the options week-by-week over the subsequent period July 22, 2010 to April 23, 2013 using the criterion function from Eq. (9), but optimizing only more than the state vector. This out-of-sample period contains quotes for more than 100,000 separate options, representing more than 56% of the number of in-sample observations.[22] The average IV (across all options) in the out-of-sample period equals 24.17%, and the average ATM IV is 18.40%.

From Fig. 3, spot volatility filtered from model (3) in the out-of-sample period continues to provide an excellent fit to the spot volatility estimated from high-frequency returns. Thus, effectively, we decompose the factors governing the option surface into current spot volatility and a separate left jump tail factor, U. The extracted volatility states provide an excellent basis for forecasting future realized return volatility and jumps, thus freeing U to accommodate the portion of the risk premium dynamics that is not tightly related to the volatility states.

The out-of-sample fit to the option surface for the various models are summarized in Table 7. Panel A provides the overall root-mean-square error, and Panel B indicates the performance for specific regions of the surface. On the right in Panel B, the RMSE for model (3) is given, and the remaining entries provide the percentage excess RMSE of the alternative specifications relative to model (3). Thus, positive entries signify the degree to which the models perform worse than model (3) for that part of the option surface during the out-of-sample period.

The results are striking. The superiority of model (3) is more pronounced out-of-sample than in-sample. Moreover, the exponential specification for return jumps performs significantly better than the Gaussian, and two-factor models offer nontrivial improvements over one-factor representations. However, none of these more standard specifications comes close to matching the performance of model (3). Furthermore, the traditional three-factor stochastic volatility model performs comparatively poorly out-of-sample, with the two-factor model doing equally well or slightly better, reflecting some degree of in-sample overfit for the former model. Thus, a danger exists of over-parameterizing the in-sample specification, but this does not manifest itself for model (3). Moving to the individual regions of the surface, Panel B shows that model (3) outperforms every other model for each single region of the surface, so the superior out-of-sample fit is uniform. Finally, in Panel C, we fit, out-of-sample, the spot volatility far better than any of the alternative models. We conclude that the risk-neutral dynamics obtained from the in-sample period remains stable and continues to capture the salient features of the option surface dynamics beyond the estimation period.

To illustrate the type of scenarios for which the improvement of model (3) relative to the more standard one-factor Gaussian jump model, 1FGSJ, is particularly significant, Fig. 6 depicts the fit of the two models to the IV skew and term structure on two separate trading days. December 19, 2012 represents a fairly typical day with an about average skew and term structure. For this day, the fit of either model is satisfactory, and there is no major discrepancy between the two. In contrast, for September 8, 2010, the skew is elevated although the level of volatility is moderate. It represents a common occurrence in the aftermath of turbulent market conditions, in this case,

[22] The sharp increase to more than seven hundred quotes per day for the out-of-sample analysis is due to two factors. One, more options are quoted at a given tenor, thus filling gaps in the moneyness dimension. Two, the introduction of weekly options increases the number of tenors available on each day, thus enriching the data in the maturity dimension. Weekly options were introduced in 2005, but only by 2011 did the associated volume become a significant fraction (almost 20%) of the total trading volume for SPX options. As a reference, for January 1996 to December 1998, we have 158 contracts per day, and we have 490 contracts per day between January 2008 and July 2010.

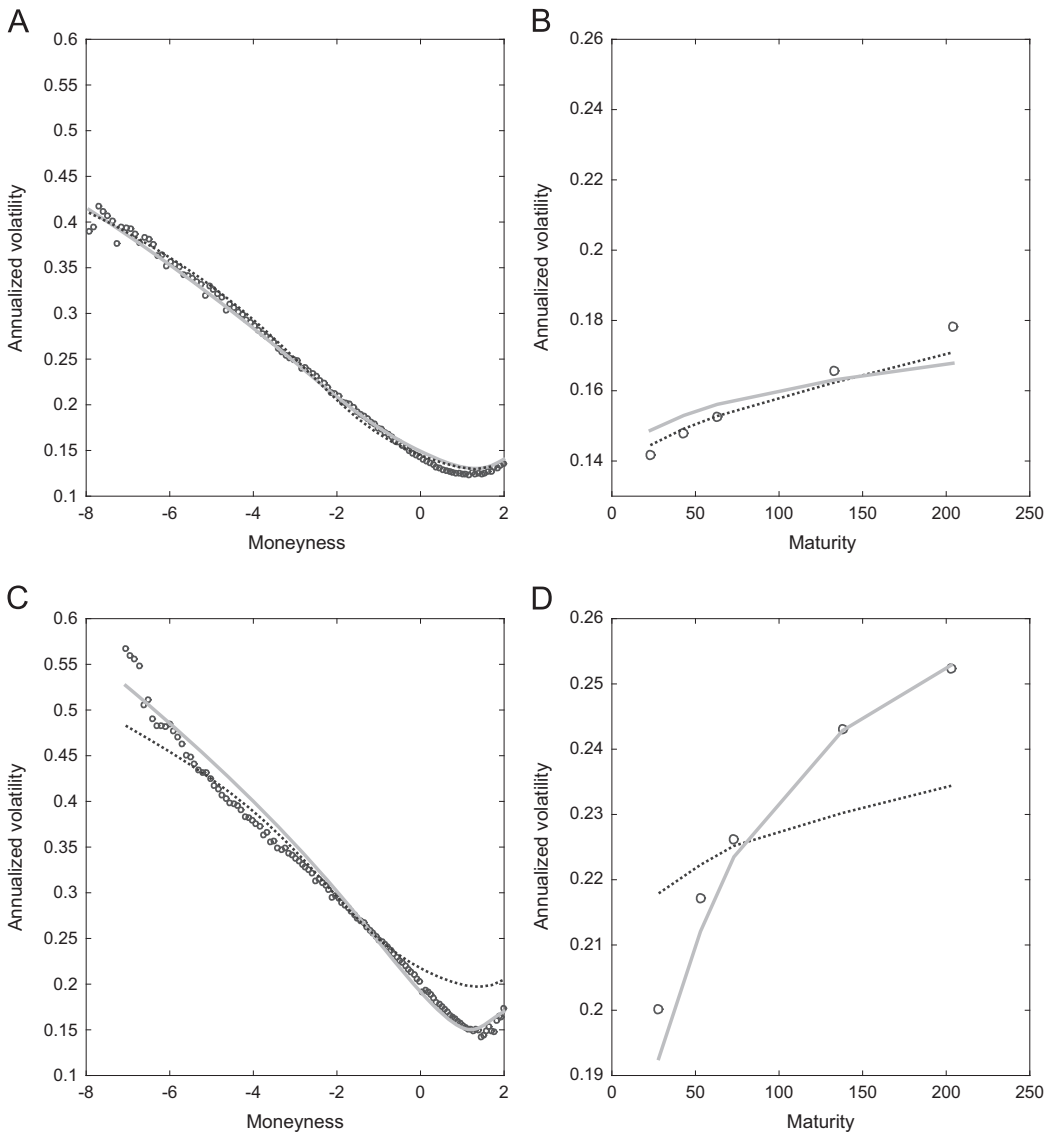

Fig. 6. Out-of-sample fit to implied volatility (IV) skew and term structure. The figure plots the fit to the IV skew and term structure for the trading days December 19, 2012 (Panels A and B) and September 8, 2010 (Panels C and D). The circles represent the observed Black-Scholes implied volatilities, the continuous line is the fit from model 3F, and the dashed line is the fit from model 1FGSJ.

associated with the initial European sovereign debt crisis. On this date, the one-factor model misses the ATM IV level badly, and it provides a very poor fit to the term structure. The problem is that the steep skew can be accommodated only through a high jump intensity, which, in the standard model, is feasible only if volatility is high. Hence, the fit to the ATM volatility is sacrificed to fit the OTM put options. Moreover, at an elevated volatility level, the mean-reversion in volatility prevents the term structure from being sufficiently steep.[23] In contrast, with the flexibility afforded by U, model (3) can readily accommodate a persistent state with an elevated intensity for the left jump tail. Furthermore, the cross-excitation between jumps and volatility is sufficient to generate an increase in the expected return variation over time, thus adapting to the relatively steep slope of the term structure.

The key to the success of our model is the severance of the linkage between jump intensity and volatility, which is, a priori, imposed in most prior work, as discussed in Section 3. In using standard models for the analysis of risk premia, one will inevitably treat the systematic mispricing of the IV skew and term structure, shown in Panels C and D of Fig. 6, as persistent observation error. This problem is recurring. Throughout the in-sample period, we observe similar qualitative developments following the Asian and Russian crises and the 2008–2009 financial crisis, while for the out-of-sample period, the second round of the European debt crisis in late 2011 also generates this type of

[23] We have confirmed that identical problems plague, e.g., the 2FESJ model in this type of scenario.

persistent dynamic in the surface. Hence, using the standard modeling framework induces systematic biases in the inference for risk premia.

7. Risk premia dynamics and predictability

This section relates our findings based on the option panel to the underlying return data. We study the links between the state vector, or risk factors, extracted from the option panel and the volatility and jump risks inferred from the underlying stock returns. This sets the stage for direct exploration of the equity and variance risk premiums and their association with the option-implied factors. Given our analysis, we rely on model (3) for tracking the IV surface dynamics. We continue to avoid making strong assumptions regarding the evolution of the actual market risks. Consequently, this part of our analysis is fully nonparametric, and we invoke only minimal stationarity conditions regarding the $\mathbb{P}$-law.

7.1. Connecting the information in the option panel and the underlying asset

To define risk premia, we must develop consistent notation concerning the pricing of each source of risk in model (3). We define

$$W^{\mathbb{P}}_{1,t} = W^{\mathbb{Q}}_{1,t} - \int_0^t \lambda^{W_1}_s\, ds, \quad W^{\mathbb{P}}_{2,t} = W^{\mathbb{Q}}_{2,t} - \int_0^t \lambda^{W_2}_s\, ds,$$
$$B^{\mathbb{P}}_{1,t} = B^{\mathbb{Q}}_{1,t} - \int_0^t \lambda^{B_1}_s\, ds, \quad B^{\mathbb{P}}_{2,t} = B^{\mathbb{Q}}_{2,t} - \int_0^t \lambda^{B_2}_s\, ds, \tag{10}$$

where $W^{\mathbb{P}}_{1,t}$, $W^{\mathbb{P}}_{2,t}$, $B^{\mathbb{P}}_{1,t}$, and $B^{\mathbb{P}}_{2,t}$ are $\mathbb{P}$ Brownian motions and $\lambda^{W_1}_t$, $\lambda^{W_2}_t$, $\lambda^{B_1}_t$, and $\lambda^{B_2}_t$ denote the associated prices of risk. The compensator of the jump measure, μ, under the $\mathbb{P}$ measure is given by $dt \otimes \nu^{\mathbb{P}}_t(dx,dy)$, and the mapping $\nu^{\mathbb{P}}_t(dx,dy) \to \nu^{\mathbb{Q}}_t(dx,dy)$, defined for every jump size x and y and every time t, reflects the compensation for jump risk.

The dynamics of the stock price process under the physical probability measure $\mathbb{P}$ is then

$$\frac{dX_t}{X_{t-}} = \alpha_t\, dt + \sqrt{V_{1,t}}\, dW^{\mathbb{P}}_{1,t} + \sqrt{V_{2,t}}\, dW^{\mathbb{P}}_{2,t} + \int_{\mathbb{R}^2} (e^x - 1)\tilde{\mu}^{\mathbb{P}}(dt,dx,dy), \tag{11}$$

where

$$\alpha_t - (r_t - \delta_t) = \lambda^{W_1}_t \sqrt{V_{1,t}} + \lambda^{W_2}_t \sqrt{V_{2,t}} + \int_{\mathbb{R}^2} (e^x - 1)\nu^{\mathbb{P}}_t(dx,dy) - \int_{\mathbb{R}^2} (e^x - 1)\nu^{\mathbb{Q}}_t(dx,dy) \tag{12}$$

is the spot equity risk premium, reflecting compensation for diffusive and (price) jump risks.

The conditional cum-dividend equity risk premium over the horizon τ is thus given by

$$\mathrm{ERP}^{\tau}_t \equiv \frac{1}{\tau}\mathbb{E}^{\mathbb{P}}_t\left(\int_t^{t+\tau} (\alpha_s - (r_s - \delta_s))\, ds\right).^{24} \tag{13}$$

We next define the quadratic variation over $[t, t+\tau]$, which we denote $QV_{t,t+\tau}$. It captures the return variation over the given horizon and is given by

$$QV_{t,t+\tau} = QV^c_{t,t+\tau} + QV^j_{t,t+\tau},$$
$$QV^c_{t,t+\tau} = \int_t^{t+\tau} (V_{1,s} + V_{2,s})\, ds, \quad QV^j_{t,t+\tau} = \int_t^{t+\tau}\int_{\mathbb{R}^2} x^2 \mu(ds,dx,dy), \tag{14}$$

where we decompose the return variation into terms generated by the continuous and jump component of X, $QV^c_{t,t+\tau}$, and $QV^j_{t,t+\tau}$. Further, the quadratic variation is independent of the probability measure. The variance risk premium is defined as

$$\mathrm{VRP}^{\tau}_t \equiv \frac{1}{\tau}\left[\mathbb{E}^{\mathbb{P}}_t\left(QV_{t,t+\tau}\right) - \mathbb{E}^{\mathbb{Q}}_t\left(QV_{t,t+\tau}\right)\right] \tag{15}$$

and is compensation for the variance risk in X.

We are also interested in assessing directly the risks and risk premiums associated with jumps. We want to gauge the compensation for large price jumps and to allow for a separate risk premium for the negative versus positive jumps. We obtain direct measures of the jump risks by simply counting the number of big jumps over the relevant horizon:

$$LT^K_{t,t+\tau} \equiv \int_t^{t+\tau}\int_{\mathbb{R}^2} 1_{\{x \le -K\}}\mu(ds,dx,dy), \quad RT^K_{t,t+\tau} \equiv \int_t^{t+\tau}\int_{\mathbb{R}^2} 1_{\{x \ge K\}}\mu(ds,dx,dy), \tag{16}$$

where K is a prespecified threshold. We set $K = 0.5\%$ in the subsequent analysis.[25]

The risk measures we have introduced, including $QV^c_{t,t+\tau}$, $QV^j_{t,t+\tau}$, $LT^K_{t,t+\tau}$, and $RT^K_{t,t+\tau}$, are not directly observable, but we can estimate them using high-frequency and overnight futures returns. Naturally, because intraday data are available only during active trading, our high-frequency measures pertain exclusively to the trading intervals within $[t, t+\tau]$. We denote them with superscript i (for intraday based measures, e.g., $QV^i_{t,t+\tau} = \sum_{s=t}^{t-1+\tau} QV_{s+\pi,s+1}$, where π denotes the fraction of the day corresponding to the overnight period and $1-\pi$ indicates the length of the trading day. $QV^{c,i}_{t,t+\tau}$, $QV^{j,i}_{t,t+\tau}$, $LT^{K,i}_{t,t+\tau}$, and $RT^{K,i}_{t,t+\tau}$ are defined analogously. By now, there are standard methods for constructing estimates for these risk measures as well as the corresponding equity and variance risk premia. We provide the details regarding our empirical implementation in the Appendix.

[24] Because a long position in the market index involves a commitment of capital, a part of the wedge in the $\mathbb{P}$ and $\mathbb{Q}$ expectations of the cum-dividend equity returns reflects compensation for the time variation in the risk-free rate. This term is absent if we instead define the equity risk premium using futures on the market index.

[25] This (fixed) threshold K is large enough that we can separate returns exceeding this (absolute) level from diffusive volatility using one-minute observations. Experiments with alternative cutoffs produced similar results.

7.2. The predictability of equity and variance risk and risk premia

We now explore the relation between the option-implied factors, V_1, V_2, and U, driving the option surface dynamics and the various risk measures and risk premia associated with the underlying asset. We rely on alternative versions of the following predictive regression:

$$y_t = \alpha_0 + \alpha_1 V_{1,t} + \alpha_2 V_{2,t} + \alpha_3 U_t + \epsilon_t, \tag{17}$$

where the left-hand-side represents, in turn, the empirical jump and diffusive variance risk measures and the risk premia, i.e., $y_t = \widehat{LT}^{K,i}_{t,t+\tau}$, $\widehat{RT}^{K,i}_{t,t+\tau}$, $\widehat{QV}^{c,i}_{t,t+\tau}$, $\widehat{QV}_{t,t+\tau}$, $\log(X_{t+\tau}/X_t) - (1/\tau)\int_t^{t+\tau}(r_s - \delta_s)\,ds$, and $\widehat{\mathrm{VRP}}^{\tau}_t$. Given the relations explicated in Appendix B, it is evident that the regressions based on the alternative y_t variables, asymptotically in sample size, yield estimates identical to those based on the corresponding infeasible measures of interest, i.e., $\sum_{s=t}^{t-1+\tau}\int_{s+\pi}^{s+1}\int_{\mathbb{R}} 1_{\{x \le -K\}}\nu^{\mathbb{P}}_s(dx,dy)$, $\sum_{s=t}^{t-1+\tau}\int_{s+\pi}^{s+1}\int_{\mathbb{R}} 1_{\{x \ge K\}}\nu^{\mathbb{P}}_s(dx,dy)$, $QV^{c,i}_{t,t+\tau}$, $QV_{t,t+\tau}$, ERP^{τ}_t, and VRP^{τ}_t. Thus, the predictive regression in Eq. (17) speaks directly to the linkages between the option surface dynamics and the risks and risk premia associated with the equity index.

In general, if the premia for the diffusive and jump risks are spanned by the factors V_1, V_2, and U, then the expectation of y_t conditional on time t information will be functionally related to $V_{1,t}$, $V_{2,t}$, and U_t. Moreover, in the standard case, almost universally adopted in option pricing applications, the measure change preserves the affine structure, so the conditional mean of y_t is linear in $V_{1,t}$, $V_{2,t}$, and U_t. Hence, the regression in Eq. (17) produces optimal (mean-square error) predictors for the volatility and jump risks at time t. Furthermore, conceptually, our extraction of $V_{1,t}$, $V_{2,t}$, and U_t provides a richer information set for forecasting the volatility and jump realizations than the history of underlying asset returns, which, at best, generates estimates of the path for $\{V_{1,s}+V_{2,s}\}_{s\le t}$ as well as associated jump variation measures.

We summarize the results from the predictive regressions in Figs. 7 and 8. Because we are particularly interested in the incremental role of the novel factor U, we initially project U linearly onto the two volatility factors and denote the residual by $\tilde{U}$. Consequently, $\tilde{U}$ reflects the features of the system not associated with the traditional volatility factors. Given our relatively short sample, we compute the predictive regressions for horizons up to one year only. Fig. 7 shows that the state variables, extracted from the option panel, have significant explanatory power for the future evolution of risks. In particular, the plot pertaining to the count of positive and negative jumps reveals that the jump intensities display highly predictable time variation under the statistical measure, $\mathbb{P}$, i.e., $\nu^{\mathbb{P}}_t(dx,dy)$ is truly a function of t. Moreover, the state variables differ greatly in their ability to forecast the future volatility and jump intensity. Once we control for the volatility factors, $\tilde{U}$ provides no incremental explanatory power. This is evident both from the insignificant t-statistics corresponding to $\tilde{U}$ and the trivial drop in R^2 when we exclude $\tilde{U}$ from the regressions. Hence, Fig. 7 is consistent with a model for which the jump intensity, under $\mathbb{P}$, depends only on the volatility factors V_1 and V_2, but not $\tilde{U}$.[26] Finally, because the empirical detection of jumps inevitably is subject to some degree of measurement error and is infeasible during the overnight period, we also display the predictability regarding the combined quadratic return variation. Because the jump and overnight return variation is less predictable, the overall explanatory power drops slightly relative to the results for the continuous variation, but the qualitative pattern is identical. In short, the distinct return variation components are highly predictable, yet the forecast power of $\tilde{U}$ is insignificant across all alternative constellations. The lack of statistical significance does not imply that U has no impact on the $\mathbb{P}$ dynamics of volatility and jump risks, but rather that the effect is marginal compared with that of the volatility factors.

We now turn to the predictability of the equity and variance risk premia. Fig. 8 indicates that our three factors, extracted from the option panel, now take on very different roles. A significant part of the predictability of both the equity and variance risk premia is due to the U factor. For the variance risk premia, V_1 also contributes strongly at shorter horizons, while, importantly, for the equity risk premium, $\tilde{U}$ is the single dominant explanatory factor for all horizons. The importance of U for predicting both the equity and variance risk premia is consistent with Bollerslev and Todorov (2011), who find the equity and variance risk premia to embed a common component stemming from compensation of left jump tail risk. The fact that both the equity and variance risk premia depend on U, coupled with the significant persistence of the U factor, rationalizes the predictive power of the variance risk premium for future excess returns, shown in Bollerslev, Tauchen, and Zhou (2009) and Drechsler and Yaron (2011). The limited role for the two volatility factors mirrors the conclusions of many prior studies on the risk-return trade-off, going back to, e.g., French, Schwert, and Stambaugh (1987) and Glosten, Jaganathan, and Runkle (1993). Finally, we note that our results are not driven by the events surrounding the financial crisis. Qualitatively identical results apply for subsamples that end prior to 2007.[27]

Another way to gauge the importance of U, and proper model specification in general, for predicting the equity and variance risk premia is to contrast our evidence to findings generated by standard jump-diffusive models. Because the results are entirely consistent with our prior conclusions, we briefly summarize the results and refer to the Supplementary Appendix for details. If we omit U from the model, we are still left with an elaborate model that, besides the two volatility state variables driving the dynamics of the option surface, incorporates diffusive and jump leverage effects, co-jumps in returns and volatility, and separates decay rates for the left and right

[26] In general, because V_1 contains jumps of time-varying intensity that load on all the factors, V_1, V_2, and U, the conditional forecast of future volatility $V_{1,t}+V_{2,t}$ still depends (critically) on the current value of the third factor U.

[27] The documentation of these results is available upon request.

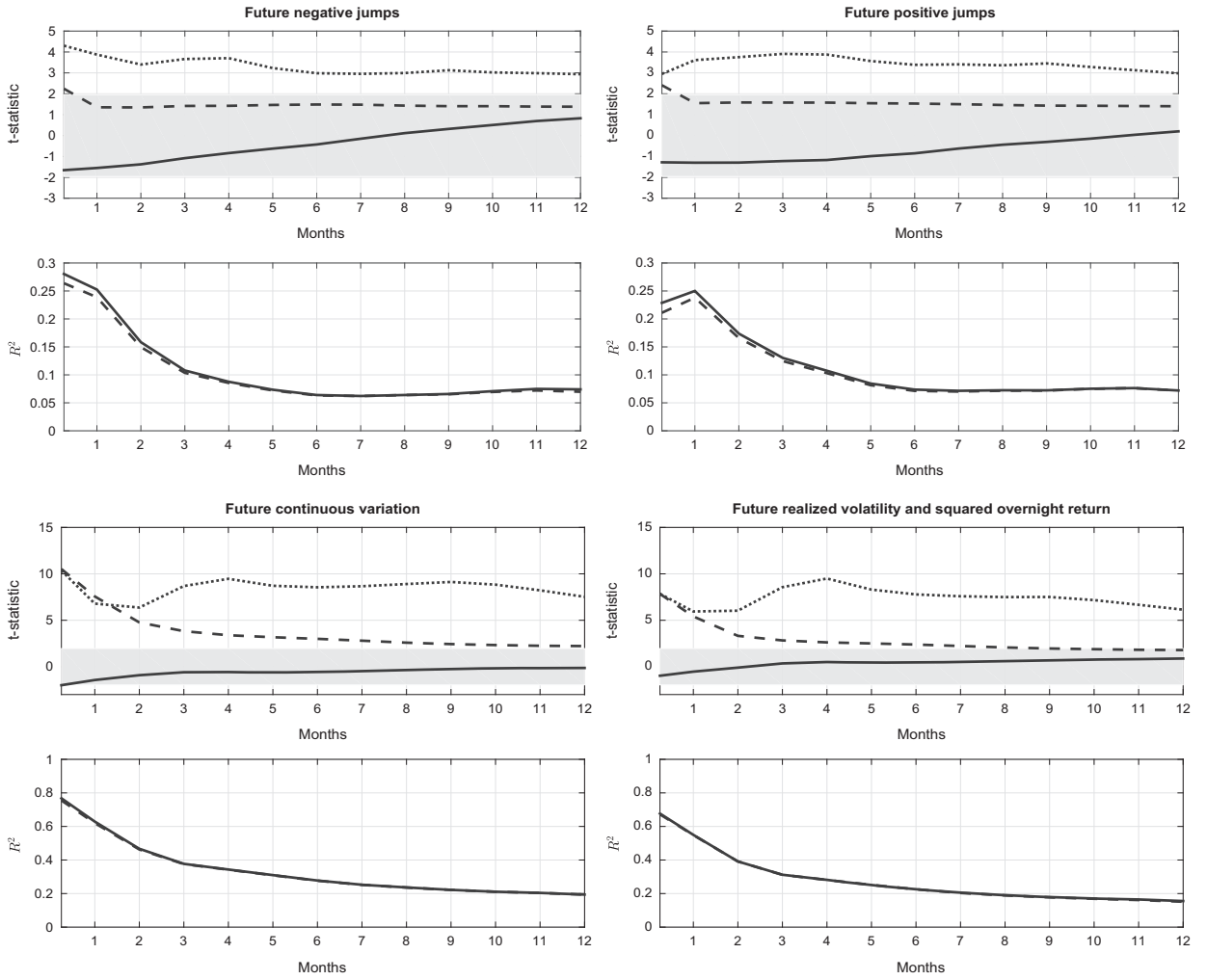

Fig. 7. Predictive regressions for volatility and jump risks. The volatility and jump risk measures are defined in Eqs. (20)–(21). For each regression, the top graph depicts the t-statistics for the individual parameter estimates, and the bottom graph indicates the regression R^2. The predictive variables are V_1 (dashed-dotted line), V_2 (dashed line), and $\tilde{U}$ (solid line), where $\tilde{U}$ is the residual from the linear projection of U on V_1 and V_2. The regression standard errors are constructed to also account for the estimation error in the projection generating $\tilde{U}$. The dashed lines in the R^2 plots correspond to constrained regressions, including only V_1 and V_2.

(exponential) jump tails.[28] The forecast performance regarding the future evolution of volatility and jump risks is similar to the corresponding results in Fig. 7. Given that $\tilde{U}$ plays only a minimal role in forecasting these quantities within model (3), this is intuitive. Moreover, as before, when considering the equity risk premium, the volatility factors are largely insignificant (and as likely to be negative as positive), and the R^2 of the predictive regression for the future excess returns is dramatically reduced. In short, the evidence for predictability of the equity risk premium vanishes when the option surface dynamics is modeled in the common jump-diffusive framework and driven exclusively by volatility factors. Hence, the inclusion of the U factor, allowing for the left risk-neutral tail to have a separate source of variation, is pivotal for capturing the predictability in the equity risk premium. Finally, for the variance risk premium, both volatility factors are significant in the two-factor model, but the R^2 of the variance risk premium regression is notably lower than for our three-factor model (3).

To summarize, consistent with prior findings, we show a substantial time variation in the pricing of market risks. However, in a key departure from existing work, we provide strong evidence that the factors driving risks and risk premia differ in a systematic way. This is ruled out, a priori, through the structure preserving measure transformations adopted in most prior option pricing studies. Thus, our results point toward the importance of allowing for nonlinearities in the pricing kernel and have implications for the ability of structural economic models to rationalize the predictability of the equity and variance risk premia.

[28] The corresponding two-factor model with Gaussian jumps performs less well along all dimensions.

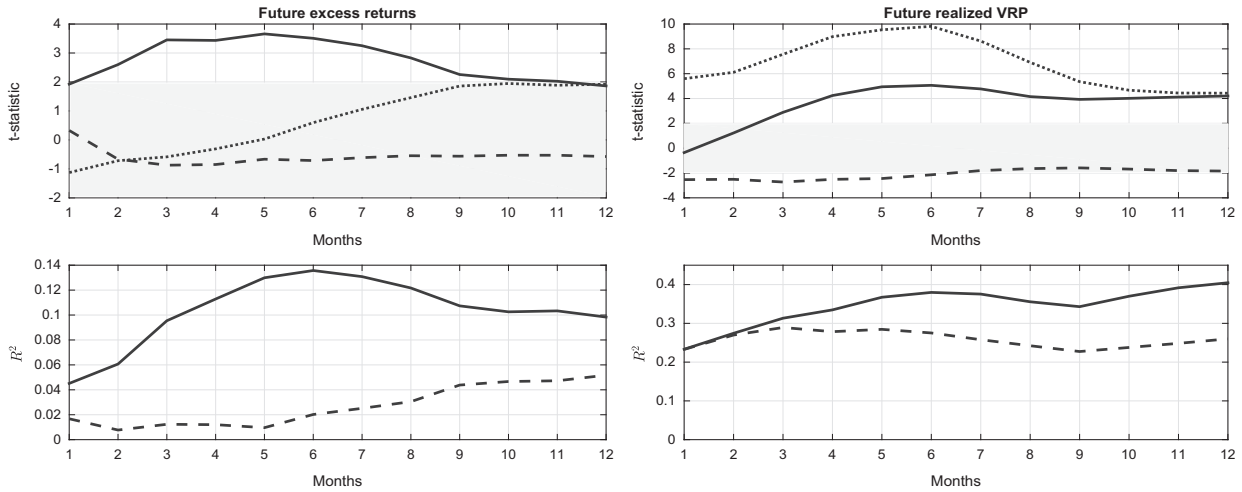

Fig. 8. Predictive regressions for equity and variance risk premia. For each regression, the top graph depicts the t-statistics for the individual parameter estimates and the bottom graph indicates the regression R^2. The predictive variables are V_1 (dashed-dotted line), V_2 (dashed line), and $\tilde{U}$ (solid line), where $\tilde{U}$ is the residual from the linear projection of U on V_1 and V_2. The regression standard errors are constructed to also account for the estimation error in the projection generating $\tilde{U}$. The dashed lines in the R^2 plots correspond to constrained regressions, including only V_1 and V_2.

7.3. Structural implications of the predictive power of the option surface

Figs. 7 and 8 demonstrate that the factor U, driving a substantial part of the OTM short maturity put option dynamics, has no impact on the actual volatility and jump dynamics of the underlying asset. In contrast, the factor has a critical effect on the pricing of volatility and jump risk. In other words, it resembles a risk premium and not a risk factor. Can this finding be rationalized from an economic perspective? To guide intuition, we compare the findings in Figs. 7 and 8 with those from recent structural models that link option prices to fundamental macroeconomic risks, such as aggregate consumption and dividends. This emerging literature has made important progress in tackling the challenging, yet critical, task of jointly explaining the equity return and risk premium dynamics in a coherent general equilibrium setting. For concreteness, we initially explore a couple of specific models featuring a representative agent with Epstein-Zin preferences exposed to risks in real consumption growth, namely, Wachter (2013) and Drechsler and Yaron (2011).

In the one-factor model of Wachter (2013), the consumption growth is subject to infrequent, but large, negative jumps (rare disasters) with a time-varying arrival rate, resembling the mechanism in Gabaix (2012).[29] This type of equilibrium model can account for many critical empirical features such as the correlation between volatility and jump risks, the time-varying jump arrival, and the ability of the market variance risk premium to predict future equity excess returns.

The model of Drechsler and Yaron (2011) specifies consumption growth as conditionally Gaussian with a time-varying conditional mean (long-run risk) and conditional volatility.[30] The system has three factors, with one driving the conditional mean and two governing the conditional volatility of consumption growth.[31] Drechsler and Yaron (2011) show that the time-varying jump intensity, in turn governed by the volatility state, explains a significant part of the predictability in the variance risk premia of future excess returns.

Figs. 9 and 10 summarize the findings from predictive regressions for future volatility and jump risks as well as equity and variance risk premia in the models of Wachter (2013) and Drechsler and Yaron (2011), using the concurrent level of the relevant state variables in each model as predictors. Not surprisingly, given the one-factor structure, the Wachter (2013) model faces some challenges in accommodating the evidence laid out in Figs. 7 and 8. Important for our analysis, the predictability of future excess returns and variance risk premia is linked closely to the predictability of the future return variation, the underlying pattern of significance is identical in all cases (flat line), and the degree of explanatory power rises roughly linearly with maturity. Compared with Fig. 7, the predictability in the Wachter (2013) model is inverted, as the return variation is forecast with relatively higher precision over long instead of short horizons. Furthermore, the explanatory power is uniformly too low. Likewise,

[29] These papers generalize work by Barro (2006) and Barro and Ursua (2008) in which rare disasters are independent and identically distributed.

[30] This model builds on Eraker and Shaliastovich (2008) and generalizes many prior models in which consumption growth contains a small predictable persistent component, including the original work of Bansal and Yaron (2004).

[31] One of the state variables that we label volatility factors directly controls the conditional variance of consumption growth, and the other captures the variation in the long-run variance of consumption growth.

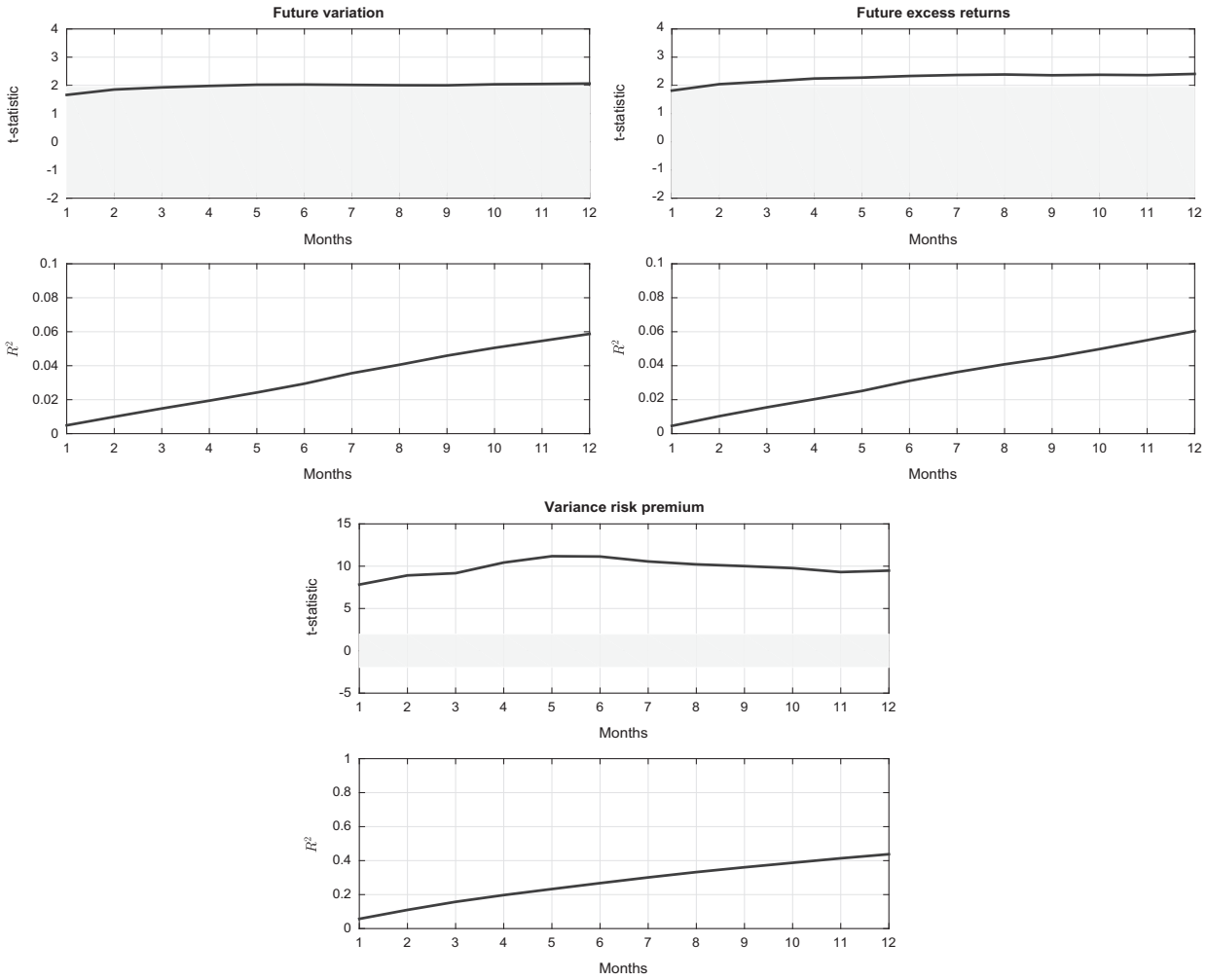

Fig. 9. Predictive regressions implied by the Wachter (2013) structural model. The predictive variable is the time-varying intensity of a rare disaster in consumption growth.

referencing Fig. 8, the model fails to capture the degree and pattern of predictability in the excess returns and variance risk premium.[32]

Turning to Fig. 10, it is evident that the more flexible volatility structure of Drechsler and Yaron (2011) is useful in accommodating some of the stylized features of the data. Nonetheless, it is equally clear that the long-run risk factor helps predict neither the future volatility and jump risks nor the equity and variance risk premia. In this structural setting, essentially all predictability stems from the two volatility factors. They provide the channel through which past variance risk premia generate predictable movements in the equity risk premium. Thus, relative to our empirical finding, captured by Figs. 7 and 8, this structural model also ties the predictability of future volatility and jump risks too closely to the predictability of the equity and variance risk premia. Equivalently, the structural model implies a tight relation between the dynamics of the option panel and the return dynamics of the underlying equity market. In contrast, our empirical results based on model (3) show a partial, and critical, decoupling between the factors driving the equity return dynamics and those governing the pricing of risk and, thus, the equity and variance risk premia.

There is a fundamental reason behind the discrepancy between our empirical findings and the implications of the structural models of Wachter (2013) and its extension in Seo and Wachter (2013), as well as Drechsler and Yaron (2011). Although the models generate risk premia through different channels — the presence of rare disasters and uncertainty about their arrival (Wachter, 2013; Seo and Wachter, 2013) versus long-run risk and stochastic volatility in consumption growth (Drechsler and Yaron, 2011) — they share a critical feature in the pricing of jump tail risk. They both imply that the ratio $\nu_t^{\mathbb{Q}}(dx,dy)/\ \nu_t^{\mathbb{P}}(dx,dy)$ is time-invariant. That is, the risk-neutral jump intensity is proportional to that under the actual probability measure,

[32] A two-factor extension, such as in Seo and Wachter (2013), in which rare disaster probability is driven by two factors, can generate dynamic patterns more consistent with the data. However, as we discuss later in more general terms, such an extension still produces a close link between the predictability of future risks and risk premia unlike what we find in the data.

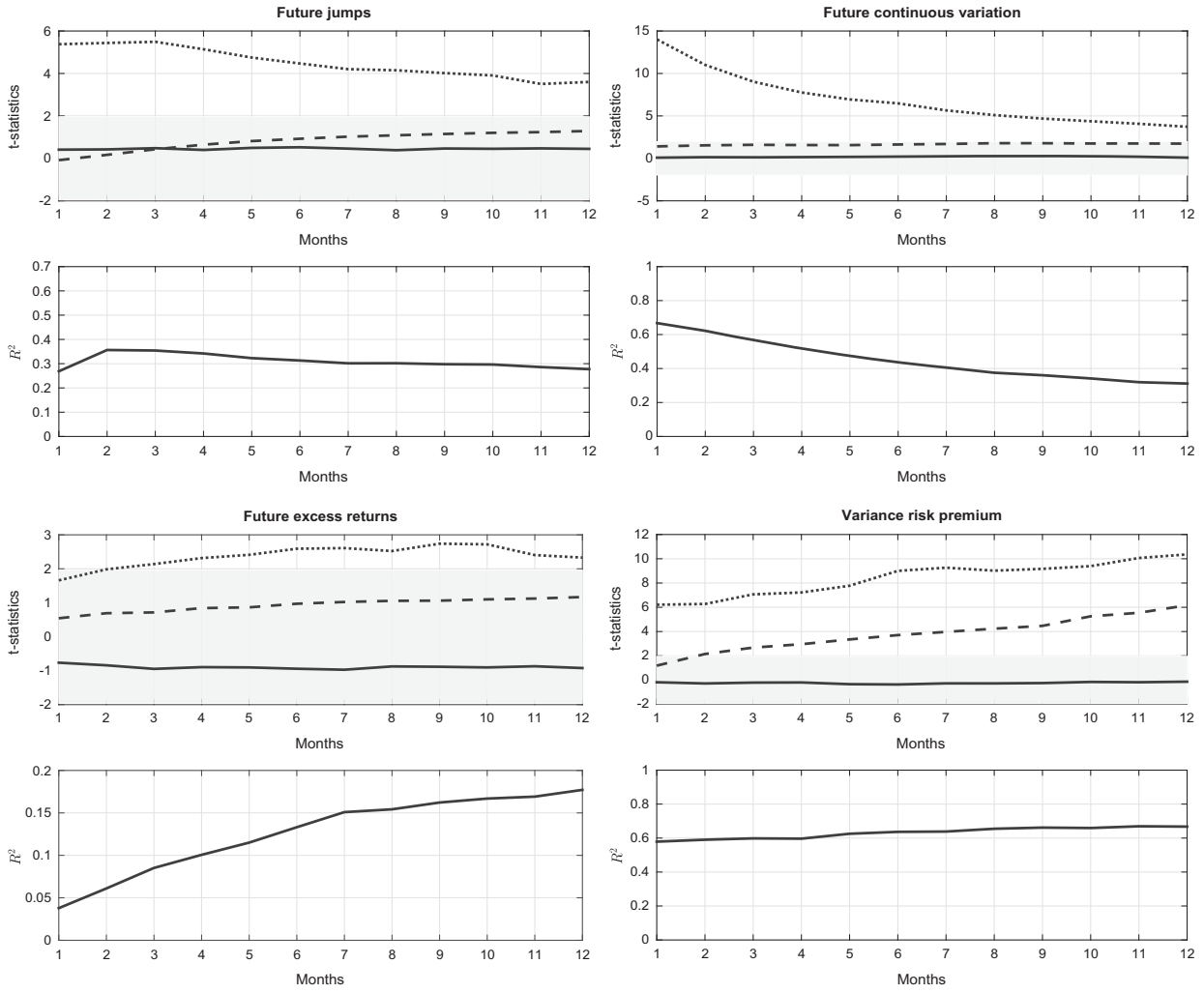

Fig. 10. Predictive regressions implied by the Drechsler and Yaron (2011) structural model. The predictive variables are the conditional mean of consumption growth (solid line), stochastic volatility of consumption growth (dotted line), and central tendency of stochastic volatility (dashed line). The dashed lines in the R^2 plots correspond to constrained regressions including only the volatility state variables.

so the two jump intensities are equivalent in terms of their time variation. Therefore, the jump risk premia are generated by changing the distribution of the jump size only. This implies that the variation in the jump intensity is inherited under the equivalent change of measure. Consequently, these equilibrium based pricing kernels cannot generate new state variables in addition to those that drive the fundamental risks in the economy. In turn, this necessarily generates the tight link between the dynamics of the underlying asset and the option surface within these models.

In fact, this tight linkage of the physical and risk-neutral jump intensities is operative for a wide class of popular structural models with representative agents having Epstein-Zin preferences. The part of the density $d\mathbb{Q}/d\mathbb{P}$ due to the change of the jump measure is characterized by

$$\mathcal{E}\left(\int_0^t \int_{\mathbb{R}^n} (Y(\omega,s,\mathbf{x})-1)\tilde{\mu}^{\mathbb{P}}(ds,d\mathbf{x})\right), \tag{18}$$

where the jump component of the state vector in the economy under the $\mathbb{P}$ probability measure is given as a (multivariate) integral of the form $\int_0^t \int_{\mathbb{R}^n} \mathbf{x}\,\tilde{\mu}^{\mathbb{P}}(ds,d\mathbf{x})$, while $Y(\omega,t,\mathbf{x}) = \nu_t^{\mathbb{Q}}(d\mathbf{x})/\nu_t^{\mathbb{P}}(d\mathbf{x})$ is the measure change for the jump intensity, and $\mathcal{E}$ is the Doléans-Dade exponential.[33] In general, $Y(\omega,t,\mathbf{x})$ will be stochastic. However, within an equilibrium setting, stipulating an affine dynamics for the fundamentals along with a representative agent with Epstein-Zin preferences generates the restriction that the expression in (18) is exponentially affine in the state vector, see, e.g., Eq. (2.22) of Eraker and Shaliastovich (2008). In turn, this implies that $Y(\omega,s,\mathbf{x})$ must be non-random and time-invariant, i.e., depend only on $\mathbf{x}$.[34] Hence, the equilibrium implied statistical and risk-neutral intensities of the price and volatility jumps

[33] For the expression in Eq. (18) and the definition of the Doléans-Dade exponential, see Jacod and Shiryaev (2003), Corollary III.5.22 and I.4.59, respectively.

[34] The restriction on $Y(\omega,s,\mathbf{x})$ is stronger. In the equilibrium model, $Y(\omega,s,\mathbf{x})$ is an exponential function of jump size; see Theorem 1 of Eraker and Shaliastovich (2008). Hence, the jump measure change is implemented by exponential tilting (in Laplace transform space), with the

(which are mixtures of the jumps in the state variables driving the fundamentals in the equilibrium model) will be affine functions of the same state vector.[35] In contrast, for our extended three-factor model, in which $\nu_t^{\mathbb{P}}(\cdot)$ loads, at most, very marginally on U_{t-}, a natural wedge exists between the time variation in statistical and risk-neutral jump intensities.

The link between the asset and option price dynamics can be relaxed in several ways within a representative agent equilibrium setting to potentially account for our empirical evidence. They all involve generalizing the preferences in some form. One approach is to allow the representative agent's coefficient of risk aversion to vary over time. Du (2010) proposes a generalization of a habit formation model in which consumption growth is independent and identically distributed with rare jumps, building on the equilibrium models of Campbell and Cochrane (1999) and Barro (2006). In this model, and consistent with our findings, a wedge emerges between the time variation of the $\mathbb{P}$ and $\mathbb{Q}$ jump intensities of the market return distribution. The nonlinearity of the pricing kernel amplifies the effect of time-varying risk aversion on the risk-neutral jump intensity relative to the statistical one. The risk-neutral jump intensity is nonlinearly related with volatility in this setting, and our U factor naturally serves as a proxy for such nonlinearities. Nevertheless, it remains an open question whether a model with external habit formation can decouple the option and asset price dynamics in a manner reminiscent of our empirical findings. It is also unclear whether the frequency and intensity of stock market jumps can be mapped into corresponding jumps in the consumption growth rate as implied by this model of habit formation.

A second approach to relax the link between the option and asset price dynamics is to recognize that agents do not directly observe the state vector and, therefore, need to filter the states from observables. The absence of perfect information plus aversion to ambiguity (particularly about extreme negative risks), as in Hansen and Sargent (2008), or lack of confidence in the estimate of the state vector, as in Bansal and Shaliastovich (2010), can make investors appear more risk averse than they would be in a perfect information setting. The key question is whether the ambiguity aversion or confidence risk variation can generate the required gap between the dynamics of the statistical and risk-neutral jump intensities.[36] For example, the excessively tight link between the jump intensity under $\mathbb{P}$ and $\mathbb{Q}$ remains within the generalization of the Drechsler and Yaron (2011) model, developed by Drechsler (2013), in which agents are ambiguous about part of the dynamics, including the jumps in the conditional mean and variance of consumption growth. The representative agent's ambiguity drives an additional wedge between fundamental risks and asset prices and helps explain why variance risk premia have superior predictive power, relative to volatility itself, for future returns. Nonetheless, the linearity of the pricing kernel with respect to the state vector implies that no new state variable is generated going from $\mathbb{P}$ to $\mathbb{Q}$, thus ultimately rendering the model predictions incompatible with our empirical findings.

Moving beyond the strict representative agent framework, parts of the literature have also considered the potential impact of the intermediary sector for the pricing of derivative securities, particularly following crises; see, e.g., Bates (2003), Hu, Pan, and Wang (2013), and Chen, Joslin, and Ni (2014). The main intuition is that major financial shocks can impose losses on market makers and reduce their effective risk bearing capacity. Can we rationale the wedge between the factors driving the risks and the risk premia through the health of the financial sector? To informally explore this question, we relate our U factor to standard measures viewed as proxies for stress in the financial sector. We incorporate the noise (liquidity) measure of Hu, Pan, and Wang (2013), the three-month London Interbank Offered Rate (LIBOR) minus Treasury (TED) spread, and the default spread defined as the difference between Moody?s BAA and AAA bond yield indices (DFSPRD), while also controlling explicitly for volatility. In Table 8, we report the related regression results.

Interestingly, we find the noise factor of Hu, Pan, and Wang (2013) to be strongly correlated with our U factor, even after controlling for volatility. While the default spread also has relatively good explanatory power, it is highly correlated with the noise factor, and the individual t-statistics drop substantially when all the variables are included in the (multivariate) regression reported in the last column. Finally, compared with the other factors, the TED spread plays a minimal role. Overall, we conclude that the critical component of U, not correlated with volatility, arguably is associated with proxies for stress in the financial sector. Hence, our procedure, extracting risk premium information directly from the option panel, generates evidence that qualitatively conforms with prior observations in the literature. We leave further explorations along these lines to future work.

8. Conclusion

We show that the standard exponentially affine jump-diffusive specifications used in the empirical option pricing literature are incapable of fitting critical features of the option surface dynamics for the S&P 500 index, especially in scenarios involving significant shifts in the volatility smirk. We extend the risk-neutral volatility model to include a separate state variable that is crucial in capturing the time variation of priced downside tail risk. This new factor has no incremental explanatory power, beyond the traditional volatility factors, for the future evolution of volatility and jump risks. Relative to the volatility components, the new factor provides critical, and superior, information for the time variation in the equity and variance risk premia.

Our findings demonstrate that the pricing in the option market is closely integrated with the underlying asset

(*footnote continued*)
degree of tilting determined by the preference parameters of the representative agent.

[35] In the models of Wachter (2013), Seo and Wachter (2013), and Drechsler and Yaron (2011), the jump intensities are even more tightly connected, as they are directly proportional.

[36] According to the estimates for Eq. ((3), U does not covary perfectly with stochastic volatility.

Table 8
U factor and the health of the financial sector.

The table presents univariate and multivariate regressions of the *U* factor on volatility and variables that proxy for the health of the financial sector (*t*-statistics in parenthesis). *V* is the variance extracted from the time series of options panels, *Noise Factor* refers to the liquidity factor proposed by Hu, Pan, and Wang (2013), TED is the spread between the three-month London Interbank Offered Rate (LIBOR) and the Treasury yield, and DFSPRD is the difference between BAA and AAA Moodys bond yield indices.

Variable	I	II	III	IV	V	VI
Constant	2.233	0.941	2.632	−0.854	0.976	0.296
	(9.279)	(5.599)	(10.071)	(−0.854)	(5.222)	(1.016)
V	60.834				20.255	19.057
	(6.204)				(2.192)	(2.480)
Noise Factor		0.907			0.727	0.618
		(20.679)			(10.466)	(6.721)
TED			2.279			−1.043
			(4.357)			(−2.960)
DFSPRD				4.616		1.593
				(17.407)		(4.117)
R^2	0.349	0.487	0.094	0.437	0.506	0.549

market. Moreover, the option panel embodies critical information regarding equity risk pricing that cannot be extracted directly from the underlying asset price dynamics. The wedge between the two probability measures arises primarily from the varying degree of compensation for downward tail jump risk. Our results suggest that time-varying risk aversion or ambiguity aversion, or both, driven in part by the presence of large shocks, must be incorporated into structural asset pricing models if they are to explain the joint dynamics of the equity and option markets.

Appendix A. Nonparametric high frequency measures

For ease of notation, we normalize the time unit to be a day. Each day is then divided into a trading and a nontrading part and by convention a day starts with the close of trading on the previous day and ends at the closing of the following day trading period. The resulting daily interval $[t-1,t]$ is divided into $[t-1,t-1+\pi]$ overnight period and $[t-1+\pi,t]$ active part of the trading day. Over the trading part, we observe the futures price at $n+1$ equidistant times, resulting in n intraday increments, each over a time interval of length $\Delta_n \equiv (1-\pi)/n$. The intraday increments are given by $\Delta_i^{n,t} f = f_{t-1+\pi+i\Delta_n} - f_{t-1+\pi+(i-1)\Delta_n}$ for $i=1,\ldots,n$ and $t=1,\ldots,T$.

$\widehat{V}_t^{(n,m_n)}$ is a nonparametric estimator of the diffusive return variation constructed from the intraday record of the log-futures price of the underlying asset, f, as follows:

$$\widehat{V}_t^{(n,m_n)} = \frac{n}{m_n} \sum_{i=n-m_n+1}^{n} (\Delta_i^{n,t} f)^2 \, 1_{\{|\Delta_i^{n,t} f| \le \upsilon \Delta_n^{\varpi}\}}, \tag{19}$$

where $\upsilon > 0$, $\varpi \in (0,1/2)$, and m_n denotes some deterministic sequence. For $m_n/n \to 0$, $\widehat{V}_t^{(n,m_n)}$ is a consistent estimator of the spot variance at t and corresponds to the truncated variation (Mancini, 2009) computed over an asymptotically shrinking fraction of the day just prior to the option quote. In our implementation, we sample every minute over a 6.75-hour trading day, excluding the initial five minutes, resulting in $n=400$. We employ $m_n=300$ for $\widehat{V}_t^{(n,m_n)}$ in Eq. (9).

Similarly, we introduce the following measures of jump and variance risks for our analysis in Section 7:

$$\begin{cases} \widehat{LT}_{t,t+\tau}^{K,i} = \sum_{s=t+1}^{t+\tau} \sum_{i=1}^{n} 1_{\{\Delta_i^{n,s} f < -K \vee (\upsilon \Delta_n^{\varpi})\}}, \\ \widehat{RT}_{t,t+\tau}^{K,i} = \sum_{s=t+1}^{t+\tau} \sum_{i=1}^{n} 1_{\{\Delta_i^{n,t} f > K \vee (\upsilon \Delta_n^{\varpi})\}}, \end{cases} \tag{20}$$

and

$$\widehat{QV}_{t,t+\tau}^{i} = \sum_{s=t+1}^{t+\tau} \sum_{i=1}^{n} |\Delta_i^{n,t} f|^2, \quad \widehat{QV}_{t,t+\tau}^{c,i} = \sum_{s=t+1}^{t+\tau} \sum_{i=1}^{n} |\Delta_i^{n,t} f|^2 1_{\{|\Delta_i^{n,t} f| \le \upsilon \Delta_n^{\varpi}\}}, \tag{21}$$

where K is the constant jump threshold given in Eq. (16).

Under general conditions, see, e.g., Jacod (2008),

$$\widehat{LT}_{t,t+\tau}^{K,i} \xrightarrow{\mathbb{P}} LT_{t,t+\tau}^{K,i}, \quad \widehat{RT}_{t,t+\tau}^{K,i} \xrightarrow{\mathbb{P}} RT_{t,t+\tau}^{K,i}, \quad \widehat{QV}_{t,t+\tau}^{i} \xrightarrow{\mathbb{P}} QV_{t,t+\tau}^{i}, \quad \widehat{QV}_{t,t+\tau}^{c,i} \xrightarrow{\mathbb{P}} QV_{t,t+\tau}^{c,i}. \tag{22}$$

For the overnight periods within $[t,t+\tau]$, we cannot separate the diffusive volatility from jumps, and we simply estimate the total (realized) overnight variance via

$$\widehat{QV}_{t,t+\tau}^{o} = \sum_{s=t+1}^{t+\tau} \left(f_{s-1+\pi} - f_{s-1}\right)^2. \tag{23}$$

Our estimate for the total variation, $QV_{t,t+\tau}$, is then given by $\widehat{QV}_{t,t+\tau} = \widehat{QV}_{t,t+\tau}^{i} + \widehat{QV}_{t,t+\tau}^{o}$.

Theoretically, for all of the above estimators, any $\upsilon > 0$ and $\varpi \in (0,1/2)$ will work. We fix $\varpi = 0.49$. The computation of υ is more involved and takes into account the fact that volatility varies over time and displays a strong diurnal pattern over the trading day. To account for the latter, we estimate, nonparametrically, a time-of-day factor TOD_i, $i=1,\ldots,n$,

$$TOD_i = NOI_i \frac{\sum_{t=1}^{T} (\Delta_i^{n,t} f)^2 1_{\{|\Delta_i^{n,t} f| \le \overline{\upsilon} \Delta_n^{0.49}\}}}{\sum_{t=1}^{T} \sum_{j=1}^{n} (\Delta_j^{n,t} f)^2 1_{\{\Delta_j^{n,t} f \le \overline{\upsilon} \Delta_n^{0.49}\}}}, \tag{24}$$

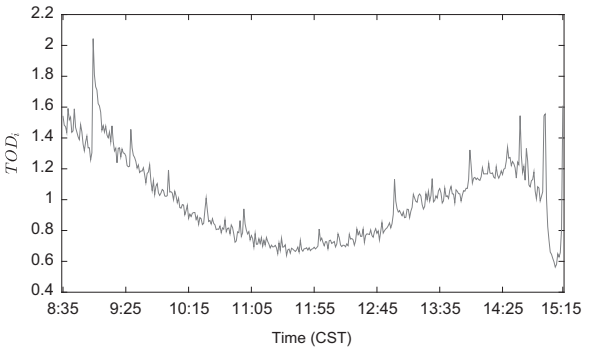

Fig. 11. Time-of-day factor, *TOD*: CST: Central Standard Time.

where $\overline{\upsilon}$ is

$$\overline{\upsilon} = 3\sqrt{\frac{\pi}{2}}\sqrt{\frac{1}{T}\sum_{t=1}^{T}\sum_{i=2}^{n}|\Delta_{i-1}^{n,t}f\,|\,\Delta_i^{n,t}f|}, \tag{25}$$

and the number of increments factor NOI_i is defined as

$$NOI_i = \frac{\sum_{t=1}^{T}\sum_{j=1}^{n} 1_{\{|\Delta_j^{n,t}f| \le \overline{\upsilon}\Delta_n^{0.49}\}}}{\sum_{t=1}^{T} 1_{\{|\Delta_i^{n,t}f| \le \overline{\upsilon}\Delta_n^{0.49}\}}}. \tag{26}$$

Eq. (26) ensures that the numerator and denominator in Eq. (24) are given in identical units. The truncation level $\overline{\upsilon}$ is based on the average in-sample volatility obtained from the bipower variation measure of Barndorff-Nielsen and Shephard (2004). The *TOD* factor is depicted in Fig. 11.

To account for time-varying volatility across days, we use the estimated continuous component of volatility for the previous day (for the first day we use $\overline{\upsilon}$). Finally, our time-varying threshold is

$$\upsilon_{t,i} = 3\sqrt{\frac{\widehat{V}_{t-1}^{n,n}}{1-\widehat{\pi}}} \times TOD_i \times \Delta_n^{0.49}, \tag{27}$$

where $\widehat{\pi}$ is given by

$$\widehat{\pi} = \frac{\sum_{t=1}^{T}(f_{t+\pi}-f_t)^2}{\sum_{t=1}^{T}(f_{t+1}-f_t)^2}. \tag{28}$$

Appendix B. Linking risks and risk premia with their feasible counterparts

From the properties of the compensator for a jump measure, we have

$$LT_{t,t+\tau}^K = \int_t^{t+\tau}\int_{\mathbb{R}^2} 1_{\{x \le -K\}}\nu_s^{\mathbb{P}}(dx,dy)\,ds + \epsilon_{t,t+\tau}^L, \quad \mathbb{E}_t^{\mathbb{P}}(\epsilon_{t,t+\tau}^L) = 0,$$
$$RT_{t,t+\tau}^K = \int_t^{t+\tau}\int_{\mathbb{R}^2} 1_{\{x \ge K\}}\nu_s^{\mathbb{P}}(dx,dy)\,ds + \epsilon_{t,t+\tau}^R, \quad \mathbb{E}_t^{\mathbb{P}}(\epsilon_{t,t+\tau}^R) = 0. \tag{29}$$

Hence, up to martingale difference sequences, $LT_{t,t+\tau}^K$ and $RT_{t,t+\tau}^K$ measure the $\mathbb{P}$ jump intensity of large jumps.[37]

Turning toward the equity and variance risk premia, we first note that, from an application of Itô formula, $\log(X_t)$ has the following representation under $\mathbb{P}$:

$$d\log(X_t) = \left[\alpha_t - q_t^{\mathbb{P}}\right]dt + \sqrt{V_{1,t}}\,dW_{1,t}^{\mathbb{P}} + \sqrt{V_{2,t}}\,dW_{2,t}^{\mathbb{P}} + \int_{\mathbb{R}^2} x\,\tilde{\mu}^{\mathbb{P}}(dt,dx,dy), \tag{30}$$

where $q_t^{\mathbb{P}} = \frac{1}{2}V_{1,t} + \frac{1}{2}V_{2,t} + \int_{\mathbb{R}^2}(e^x - 1 - x)\,\nu_t^{\mathbb{P}}(dx,dy)$ and similarly under $\mathbb{Q}$ with α_t replaced by $r_t - \delta_t$ and all superscripts $\mathbb{P}$ replaced with $\mathbb{Q}$.

Hence, we have the following relations for the feasible measures of the equity and variance risk premia:

$$\log\left(\frac{X_{t+\tau}}{X_t}\right) - \frac{1}{\tau}\int_t^{t+\tau}(r_s - \delta_s)\,ds = \mathrm{ERP}_t^\tau + \frac{1}{\tau}\mathbb{E}_t^{\mathbb{P}}\left(\int_t^{t+\tau} q_s^{\mathbb{P}}\,ds\right) + \epsilon_{t,t+\tau}^E, \quad \mathbb{E}_t^{\mathbb{P}}\left(\epsilon_{t,t+\tau}^E\right) = 0,$$
$$\widehat{\mathrm{VRP}}_t^\tau = \frac{1}{\tau}\left[\widehat{QV}_{t,t+\tau} - \mathbb{E}_t^{\mathbb{Q}}(QV_{t,t+\tau})\right] = \mathrm{VRP}_t^\tau + \epsilon_{t,t+\tau}^V, \mathbb{E}_t^{\mathbb{P}}\left(\epsilon_{t,t+\tau}^V\right) = 0 \tag{31}$$

where $\mathbb{E}_t^{\mathbb{Q}}(QV_{t,t+\tau})$ can be measured in model-free fashion via VIX. Eq. (31) shows that a martingale difference sequence separates $\widehat{\mathrm{VRP}}_t^\tau$ from VRP_t^τ and, likewise, that a martingale difference sequence separates the log excess cum-dividend returns on the underlying asset from the unobservable $\mathrm{ERP}_t^\tau + (1/\tau)\mathbb{E}_t^{\mathbb{P}}\left(\int_t^{t+\tau} q_s^{\mathbb{P}}\,ds\right)$. In principle, we can remove the term stemming from the convexity adjustment, i.e., $(1/\tau)\mathbb{E}_t^{\mathbb{P}}\left(\int_t^{t+\tau} q_s^{\mathbb{P}}\,ds\right)$, via a consistent estimator for $\int_t^{t+\tau} q_s^{\mathbb{P}}\,ds$ (again up to a martingale difference term) obtained from high-frequency data, e.g.,

$$\int_t^{t+\tau}\widehat{q}_s^{\mathbb{P}}\,ds = \sum_{i:(i/n)\in(t,t+\tau]}\left[\frac{1}{2}|\Delta_i^n f|^2\,1_{\{|\Delta_i^n f| \le \upsilon_{t,i}\}} + \left(e^{\Delta_i^n f} - 1 - \Delta_i^n f\right)1_{\{|\Delta_i^n f| > \upsilon_{t,i}\}}\right].^{38} \tag{32}$$

In practice, this adjustment is minute and the results are virtually unchanged if we implement it.[39]

Appendix C. Supplementary data

Supplementary data associated with this article can be found in the online version at http://dx.doi.org/10.1016/j.jfineco.2015.06.005.

References

Ahn, D., Dittmar, R., Gallant, A., 2002. Quadratic term structure models: theory and evidence. Review of Financial Studies 15, 243–288.
Andersen, T.G., Bondarenko, O., Gonzalez-Perez, M.T., 2015. Exploring return dynamics via corridor implied volatility, Review of Financial Studies, forthcoming.
Andersen, T.G., Fusari, N., Todorov, V., 2015. Parametric inference and dynamic state recovery from option panels. Econometrica 83, 1081–1145.
Andrews, D., 2001. Testing when a parameter is on the boundary of the maintained hypothesis. Econometrica 69, 683–734.

[37] Empirical estimates for the number of large negative and positive jumps across our sample are provided in Section C of the Supplementary Appendix.

[38] For the overnight periods, we take just one-half of the squared return.

[39] We do not report results adjusting for this term to conserve space. They are available upon request.

Bai, J., Ng, S., 2002. Determining the number of factors in approximate factor models. Econometrica 70, 191–221.
Bansal, R., Shaliastovich, I., 2010. Confidence risk and asset prices. American Economic Review 100, 537–541.
Bansal, R., Yaron, A., 2004. Risks for the long run: a potential resolution of asset pricing puzzles. Journal of Finance 59, 1481–1509.
Barndorff-Nielsen, O.E., Shephard, N., 2004. Power and bipower variation with stochastic volatility and jumps. Journal of Financial Econometrics 2, 1–37.
Barro, R., Ursua, J.F., 2008. Macroeconomic crises since 1870. Brookings Papers on Economic Activity Spring, 255–335.
Barro, R.J., 2006. Rare disasters and asset markets in the 20th century. Quarterly Journal of Economics 121, 823–866.
Bates, D.S., 1991. The crash of '87—Was it expected? the evidence from options markets. Journal of Finance 46, 1009–1044.
Bates, D.S., 2000. Post-'87 crash fears in S&P 500 future options. Journal of Econometrics 94, 181–238.
Bates, D.S., 2003. Empirical option pricing: a retrospection. Journal of Econometrics 116, 387–404.
Bates, D.S., 2012. US stock market crash risk, 1926–2010. Journal of Financial Economics 105, 229–259.
Bollerslev, T., Tauchen, G., Zhou, H., 2009. Expected stock returns and variance risk premia. Review of Financial Studies 22, 4463–4492.
Bollerslev, T., Todorov, V., 2011. Tails, fears, and risk premia. Journal of Finance 66, 2165–2211.
Bollerslev, T., Todorov, V., 2014. Time varying jump tails. Journal of Econometrics 183, 168–180.
Broadie, M., Chernov, M., Johannes, M., 2007. Specification and risk premiums: the information in S&P 500 futures options. Journal of Finance 62, 1453–1490.
Brockwell, P., 2001. Continuous-time ARMA processes. In: Shanbhag, D., Rao, C. (Eds.), Handbook of Statistics, vol. 19. North-Holland, Amsterdam.
Campbell, J., Cochrane, J., 1999. By force of habit: A consumption-based explanation of aggregate stock market behavior. Journal of Political Economy 107, 205–251.
Chen, H., Jostlin, S., Ni, S., 2014. Demand for crash insurance, intermediary constraints, and stock return predictability.
Chernozhukov, V., Hong, H., 2004. Likelihood estimation and inference in a class of non-regular econometric models. Econometrica 72, 1445–1480.
Christoffersen, P., Heston, S., Jacobs, K., 2009. The shape and term structure of the index option smirk: Why multifactor stochastic volatility models work so well. Management Science 55, 1914–1932.
Christoffersen, P., Jacobs, K., Ornthanalai, C., 2012. Dynamic jump intensities and risk premiums: evidence from S&P 500 returns and options. Journal of Financial Economics 106, 447–472.
Drechsler, I., 2013. Uncertainty, time-varying fear, and asset prices. Journal of Finance 68, 1843–1889.
Drechsler, I., Yaron, A., 2011. What's vol got to do with it? Review of Financial Studies 24, 1–45.
Du, D., 2010. General equilibrium pricing of options with habit formation and event risks. Journal of Financial Economics 99, 400–426.
Duffie, D., Filipović, D., Schachermayer, W., 2003. Affine processes and applications in finance. Annals of Applied Probability 13# (3), 984–1053.
Duffie, D., Pan, J., Singleton, K., 2000. Transform analysis and asset pricing for affine jump-diffusions. Econometrica 68, 1343–1376.
Eraker, B., Shaliastovich, I., 2008. An equilibrium guide to designing affine pricing models. Mathematical Finance 18, 519–543.
French, K., Schwert, W., Stambaugh, R., 1987. Expected stock returns and volatility. Journal of Financial Economics 19, 3–29.
Gabaix, X., 2012. Variable rare disasters: an exactly solved framework for ten puzzles in macro-finance. Quarterly Journal of Economics 127, 645–700.
Glosten, L., Jaganathan, R., Runkle, D., 1993. On the relation between the expected value and the volatility of the nominal excess return on stocks. Journal of Finance 48, 1779–1801.
Hansen, L., Sargent, T., 2008. Robustness. Princeton University Press, Princeton, NJ.
Hu, G., Pan, J., Wang, J., 2013. Noise as information for illiquidity. Journal of Finance 68, 2223–2772.
Jacod, J., 2008. Asymptotic properties of power variations and associated functionals of semimartingales. Stochastic Processes and Their Applications 118, 517–559.
Jacod, J., Shiryaev, A.N., 2003. Limit Theorems For Stochastic Processes, 2nd edition Springer-Verlag, Berlin, Germany.
Johnson, T., 2012. Equity risk premia and the VIX term structure. Unpublished working paper. Stanford University, Stanford, CA.
Kou, S., 2002. A jump diffusion model for option pricing. Management Science 48, 1086–1101.
Leippold, M., Wu, L., 2002. Asset pricing under the quadratic class. Journal of Financial and Quantitative Analysis 37, 271–295.
Mancini, C., 2009. Non-parametric threshold estimation for models with stochastic diffusion coefficient and jumps. Scandinavian J. Statistics 36, 270–296.
Merton, R., 1976. Option pricing when underlying asset returns are discontinuous. Journal of Financial Economics 3, 125–144.
Santa-Clara, P., Yan, S., 2010. Crashes, volatility, and the equity premium: lessons from S& P 500 options. Review of Economics and Statistics 92, 435–451.
Seo, S., Wachter, J.A., 2013. Option prices in a model with stochastic disaster risk. Unpublished working paper. University of Pennsylvania, Philadelphia, PA.
Wachter, J.A., 2013. Can time-varying risk of rare disasters explain aggregate stock market volatility? Journal of Finance 68, 987–1035.